Uppsala University & Utrecht University

Master Thesis Energy Science

Techno-economic analysis of seven wave energy converters and their contribution to system adequacy

A case study on Sweden and the UK

Author:
Tim van den Akker MSc.

Supervisors:
Dr. Malin Göteman (Uppsala University)
Prof. Madeleine Gibescu (Utrecht University)

January 28, 2021

UPPSALA UNIVERSITET

Universiteit Utrecht

The header image shows the floating bouy wave energy converter developed by the Swedish company CorPower, Reference: CorPower (2020)

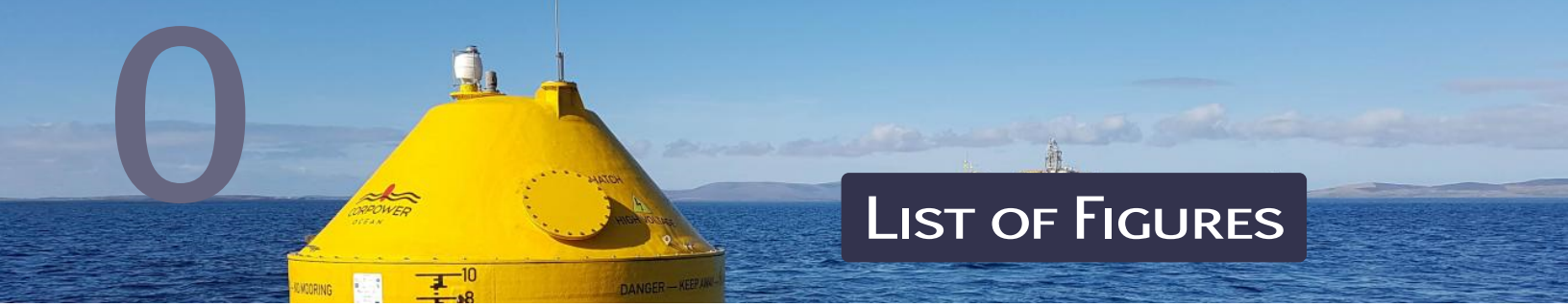

Page

Page

Abstract

Wave Energy Converters (WECs), can play a significant role in shifting energy supply from fossil-based to renewable. There is however no dominant design for an optimal WEC, likely because different WECs favour different sea states. In addition, the fact that the sector is on the verge to obtaining commercial viability, causes the WEC market to be competitive and developers to be hesitant in sharing (economical) details, leading to large uncertainties in scientific techno-economic analyses and feasibility studies. Also, feasibility can differ per location and WEC used. Wave energy is said to be less variable compared to other renewable sources like wind and solar PV. This research adds to the existing literature on the feasibility of WECs by presenting the techno-economic metrics of seven WECs in two locations, being Lysekil (Sweden) and WaveHub (the UK). In addition, the variability is compared to wind generation and solar PV. Also, the effect of integrating wave energy on system adequacy is computed by using a combination of the Z-method and the Value Adjusted Levelized Cost of Electricity (VALCOE). The resulting PBP and LCOE are higher in Lysekil compared to WaveHub. The LCOE of the WaveHub site is in range with other values found in the literature, and remains slightly above the LCOE of other renewable technologies. The variability of power output from wave energy is found to be lower than onshore and offshore wind, and solar PV, at both locations. The Z-method and VALCOE pointed out that the energy systems in both countries can safely integrate large scale WEC parks without losing system adequacy. Future research can apply the methods used on other renewable energy technologies, and test a method to value energy flexibility in the same way as capacity is treated in this research.

Plain language abstract

Electricity from ocean waves can contribute a lot to making our electricity supply fossil-free. However, there does not exist one single best device to harvest electricity from waves, because wave climates and properties differ around the globe. Due to the variety in devices, developers tend to keep economical and technical properties secret, because the market of wave energy devices is competitive. This makes scientific studies on the feasibility of wave energy devices uncertain. Also, it is often argued that wave power has a lower variability than for example wind power generation or the output from solar panels. Integrating wave power would therefore put less pressure on the electricity grid and would therefore be favourable. In this study, seven wave energy devices are considered with the wave climate of two locations, being Lysekil (Sweden) and WaveHub (the UK). For both countries, the economic feasibility was calculated, as well as the variability of the power output and the pressure it would give to integrate these devices into the electricity grid of both countries. The results of the economical analysis are in line with other calculations found in the literature, with WaveHub being a more profitable site compared to Lysekil. The variability of wave power generation is found to be lower compared to wind and solar panels, and the pressure it would provide on the electricity grids of both countries is very low.

Fossil-based energy resources, like oil and gas, are a burden on the climate system. Also, these sources are finite. Interest in sustainable energy resources has therefore grown over the past decades. One of the (many) ways of harvesting energy in a more sustainable way is by using Wave Energy Converters (WECs), used to collect the energy present in ocean- and sea waves.

Gunn and Stock-Williams (2012) found that the theoretical potential of wave power globally is 2.11 ± 0.05 TW. When using a theoretical WEC, they found that 4.6 % (0.1 TW) of this power can be extracted for final electricity use (Gunn and Stock-Williams, 2012). The total world electricity consumption was 23696 TWh in 2017 (IEA, 2020b), if evenly spread over the year, this is equivalent to 2.71 TW, showing that wave energy can play a significant role in supplying this power. Unused, the energy in the waves will be depleted by friction (internal or with the ocean floor or coastlines) and wave breaking (Falnes, 2007).

The advantages of using WECs include therefore the abundant resource, but also their low environmental impact, negligible land use and the high energy flux (Clément et al., 2002). Also, the boost it will give to a declining industry such as the offshore engineering and ship industry is mentioned as an advantage for large scale wave energy projects (Clément et al., 2002). Furthermore, since the biggest part of the WECs is either at the water surface or submerged, it could be integrated with existing offshore structures such as oil platforms (Oliveira-Pinto et al., 2019) or offshore wind turbines (Clemente et al., 2020).

Wave energy is found to be less variable compared with offshore wind power generation (Astariz and Iglesias, 2016a). Waves are said to be more predictable. Because of the linkage between wind and waves (one of the two main mechanisms of generating waves is by the wind), a peak in wind power is often followed by a peak in wave power, allowing more time to estimate the power production (Astariz and Iglesias, 2016a, Chozas et al., 2013). Also, Sheng (2019b) argues that due to the negligible energy loss waves encounter when travelling over large distances, one can quite accurately predict the energy flux in the near future.

Although there are several advantages of using WECs, it is not widely used as a sustainable energy source (Aderinto and Li, 2018). The first WEC patent was granted in 1799 (Clément et al., 2002), and in particular during the 1970s and 1980s there has been a peak in interest in wave energy, which is believed to at least partly be caused by the oil crisis in 1973 (McGlade and Ekins, 2015). Regardless of the studies done, prototypes developed and the promising potential of the energy source, other sustainable energy sources have been implemented more widely (Aderinto and Li, 2018).

In 2009, there where over a thousand different WEC designs patents present (Falcão, 2009). This is likely because different WECs favour different wave climates. The technology was 25 years after the interest peak in the 80s still in its R&D phase (Drew et al., 2009), and large scale commercial applications are rare. It is therefore uncertain for investors to back the technology. Also, there is no 'Dominant Design'. Developers of WECs are furthermore hesitant in sharing the properties of their technology, because of the competitive nature of the WEC-market.

Astariz and Iglesias (2015) summarize the main challenges for large scale implementation of wave energy to be: 1) The technology is still in an early development phase, 2) There are uncertainties about the impact of large scale wave energy projects on the coast or the marine system and 3) the technology is regarded as uneconomical. They emphasize the need for thorough

economic analyses. More techno-economic studies on different WECs might contribute to the credibility, and therefore to the development of WECs on a larger scale.

Attempts have been made to create a solid techno-economical assessment method for WECs. Teillant et al. (2012) for example tried to overcome uncertainties in operational costs, resulting from lacking operational experience, by creating a comprehensive sub-model that deals with costs during the whole operational process. Efforts on developing a method to calculate the most cost-optimal WEC design, by tuning hydro-dynamical parameters, has been done for example by Piscopo et al. (2017). A 'bottom-up' approach to assess the potential of a certain site, tested for four different WECs, has been done by Xu et al. (2020). Also the optimal size of WEC arrays has been investigated, for example by De Andres et al. (2016).
There is an abundance of site-specific wave energy research, for example in the Phillipines (Quitoras et al. (2018)), the European West Coast (O'Connor et al. (2013)), South Africa (Biyela and Cronje (2016)), and the US west coast (Chang et al. (2018b)). The most common way to conduct such an analysis is by choosing one (or a few) WEC(s), combine it with data on the wave climate on one (or a few) location(s) to compute the energy output, and finally combine the energy output with the monetary resources required for the WEC(s) to calculate economical indicators such as the Levelized Cost of Electricity (LCOE) or the Pay Back Period (PBP). The most common uncertainty in these studies is the estimation of the performance of a WEC, and its associated capital and operational costs. Since the market for WEC is still in development and therefore highly competitive, it seems hard to find reliable and complete information on the economics of a WEC.

It has been argued (for example by Chozas et al. (2013)) that wave energy is less variable than offshore wind, and therefore it is less of a burden to integrate it in the energy system, but a study that quantifies the lower variability of wave energy in monetary terms, and therefore makes it fairer to compare the LCOE of wave energy to other technologies, could not be found. There are metrics, for example developed by the IEA (see for example Graham (2018)) to give monetary values to for example a lower variability. The Value Adjusted Levelized Cost of Electricity, in parcticular the Capacity Adjustment described in IEA (2020b), offers a way of taking variability and the associated burden on the energy system in monetary terms into account.

This study focuses on the techno-economic assessment of seven different WECs, of which the properties can be found in a publication by Babarit et al. (2012). The reliability of the associated performance data, summarized in so-called 'power matrices', is tested by comparing them to similar power matrices published by other researchers and/or provided by the industry. The power matrices are used in combination with data on the wave climate of two different locations in Europe: Lysekil, which is situated on the Swedish west coast and the WaveHub project site, situated on the Northern coast of Cornwall. Lysekil has been analyzed as test site for different WEC designs (Leijon et al., 2008, Lejerskog et al., 2015), and there is an abundance of data available[1].
The main objective was to develop a model that given a certain WEC, in the form of an unique power matrix, and a location in the form of wave climate data calculates economic indicators (a.o. LCOE and the PBP) and the impact the integration of this variable renewable energy source has on the electricity grid of the country using the VALCOE as starting point. The methodology of the VALCOE, provided by IEA (2018), is very general: this research proposes a more specific method of calculating the Capacity Adjustment, and tests this method on both locations as case study. The developed VALCOE-method can easily be applied to other renewable technologies as well.

A Monte Carlo analysis is conducted on the three most important input values of the model, using the bandwidth of values found in the literature to construct probability density functions.

[1] provided by dr. Malin Göteman.

The three most important input variables are the power matrices and the investment and operational expenses, and are turned to probability density functions because of their uncertainty. For the economic indicators, the investment (referred to as 'CAPEX') and the operational expenses (referred to as 'OPEX') are needed, and their spread in value from the literature was found to be large.

The knowledge gap that this research fills is twofold: it will add a techno-economic analysis on two locations and seven WECs to the body of literature, and it will present a method to calculate the VALCOE. This study includes two extensive case studies on Sweden and the UK, and the application on a smaller energy system of Malta. The research question that guided this study is as follows:

What are the values of the techno-economic indicators of seven WECs at Lysekil and WaveHub, and what is their contribution to the system adequacy?

Typical subquestions that guided this research are:

- How do the power matrices published by Babarit et al. (2012) compare to matrices found in the other literature and/or provided by the industry?
- Which of the seven WECs is most profitable in the two locations for a given wave climate? What causes the difference?
- Is there a significant difference in calculated values of the LCOE with other sources?
- How does the integration of wave energy influence the reliability of the electricity systems of both countries? Does this differ per country? How does this relate to the variability of wave energy?
- How does the variability of wave energy compare to other sustainable energy technologies, such as offshore wind?
- What are the confidence intervals for the techno-economic and reliability indicators?

In chapter 2, the theoretical background of this study is presented. Chapter 3 summarizes the methods of processing the various sources of data, and the strategy used for the Monte Carlo analysis. Chapter 4 consists of the results, categorized per metric. In chapter 5 two more case studies are discussed: Malta and a wave park. Chapter 6 contains the Monte Carlo analysis. Chapter 7 contains the discussion of the results, and this thesis is ended with Chapter 8, the conclusion.

2 Theoretical Background

First, the theory on energy in waves is discussed. Then, the concept of harvesting power from ocean waves and the WECs used in this research is presented. Then, the steps taken from wave climate data to power production are discussed. Finally, the metrics for the economic analysis are introduced. Those economic metrics, and the corresponding abbreviations, are the Pay-back Period (PBP) and the Levelized Cost of Electricity (LCOE). For analyzing the impact the integration of a WEC, as a variable power source, on the electricity grid of the countries considered, parts of the VALCOE are used, which is introduced in this chapter as well. A short description on how the input materials would look like to compute these metrics will be given, but an extensive overview of the material sources and the way of processing will be given in the next chapter.

2.1 Energy in waves

In this research, short waves are considered, with wave periods in the order of seconds to minutes, excluding large scale waves such as the tides.

At the boundary of the ocean and the air above, referred to as the 'free surface' there exists a feedback mechanism between fluctuations in air pressure (turbulent wind) and the growing waves. The turbulent wind induces changes to the free surface, that in turn enhance the pressure fluctuations, which makes waves grow. The dominant force stopping the wave-growing mechanism is the surface tension, that provides a net force at the surface, because of the lack of water molecules above it.

There are three contributions to the energy density of waves (defined as the total energy per surface unit): 1) Kinetic energy in the movement of the surface unit, 2) potential energy due to gravity and 3) potential energy due to surface tension. Solving the energy balance shows that the energy present in waves is scaled quadratically with their amplitude.

Since wind is the main powering mechanism for wave development, more powerful waves emerge when there is a stronger wind or when the wind has a larger area of free surface to effect on, referred to as the 'fetch'. Therefore, coastlines that are exposed to unblocked oceans and/or to storm tracks will experience more powerful waves. One could expect from this fact that the WaveHub site in Cornwall has a higher energy ouput compared to Lysekil. The WaveHub site has for certain wave directions the Atlantic ocean as fetch, whereas Lysekil is situated in a sea more confined by nearby coastlines.

Due to the large variety in ocean waves, it is often practical to consider a wave spectrum, which is a statistical way of describing what the chances are of encountering a certain sea state. 'Sea state' is defined as the state of the sea at one particular moment, for a given time. It can be interpreted as a 'snapshot' of 0.5 - 3 hours. The 'wave climate' is the average of a certain amount of sea states, generally of multiple years, and can for example be expressed as a probability table for all possible sea states.

There are two methods of obtaining relevant wave climate statistics used in this research. Method one is by using Fourier analysis directly on buoy measurements. Method two is by using a data set resulting from model calculations validated with buoy measurements, (the SWAN model is used in this study, see for the documentation Booij et al. (1997)).

The theory on ocean waves and the interaction with the wind presented in this research mainly comes from academic courses with unpublished material, but the reader is referred to P. Janssen and P. A. Janssen (2004) and Salmon (2008) for an introduction on the theory on ocean waves.

2.2 Wave Energy Converters

The movement of the free surface of the ocean can be transferred to energy. The most general way a wave energy converter works is that it translates the relative motion of two bodies into electricity, by letting one of the bodies move with the waves while the other remains (semi-)static. These bodies can be for example both be at the sea surface, or bottom-fixed, or both completely submerged, as long as there is relative movement between the two bodies. The forces the two bodies exert on each other can with the help of a power take-off system (PTO), be turned to useful electricity. Examples of PTOs include springs, conductors, hydraulic mechanism and air chambers with turbines. The combinations of 'body designs' and PTOs gives many possibilities for WEC design, tuned to the wave climate the WEC needs to be deployed in.

In this research, seven WECs described in Babarit et al. (2012) are analyzed, because of the comprehensive method used in their study. Also, the matrices from Babarit et al. (2012) are used in other studies as well, for example by Oliveira-Pinto et al. (2019), which made it possible to compare results from this study to other studies to validate the calculations done. Their characteristics are summarized in Table 2.1, for a full description, the reader is referred to Babarit et al. (2012).

Table 2.1: *Summary of the WECs used in this research, from Babarit et al. (2012). Babarit et al. (2012) mention that the F-2HB analysis is inspired on the device developed by WaveBob.*

Name	**Abbreviation**	**Characteristics**	**Commercial example**
Small Bottom-referenced Heaving Buoy	*Bref-HB*	Axi-symmetric fully floating buoy, with a wire attached to a sea-floor based generator.	Seabased WEC (Seabased, 2020)
Bottom-referenced Submerged Heave Buoy	*Bref - SHB*	Same principle as the Bref-HB, only with the axi-symmetric buoy submerged under the free surface	CETO WEC (Carnegie, 2020)
Floating Two-body Heaving Converter	*F-2HB*	Moving ring around a vertical shaft, not bottom-fixed	WaveBob (bankrupt)
Bottom-fixed Heave Buoy	*B-HBA*	Several floating spheres attached to a fixed construction above the free surface but based on the sea floor	WaveStar (WaveStar, 2020)
Floating Heave-Buoy Array	*F-HBA*	Array of heaving buoys attached to a submerged, ballasted structure	Pontoon Power Converter (Pontoon, 2020)
Floating Three-body Oscillating Flap Device	*F-3OF*	Four floating hinged flaps in a rectangular shape, letting waves in from all directions. The motion of the flaps relative to the support structure is turned to usefull electricity	Langlee (Langlee, 2020)
Floating Oscillating Water Column	*F-OWC*	Fully floating device that lets incoming wave push an air column through an air turbine	Ocean Energy Ltd. (Ocean Energy Ireland, 2020)

2.3 Techno-economic metrics

In the next sections, the two main techo-economic metrics that are used in this research are introduced, as well as the parts used from the VALCOE.

2.3.1 Pay Back Period (PBP)

The pay back period is the period it takes for a project to earn itself back, meaning the time it takes for the gross income of selling the power minus the OPEX to be bigger than the CAPEX. The PBP is given in Equation 2.1, t a time step, $PO(t)$ the time-dependent power output of the device, and p_e the price of electricity. The goal of solving Equation 2.1 is to check for which time step t the inequality on the right-hand side (RHS) is satisfied. The corresponding time step t is then marked as the PBP.

$$PBP = t \leftrightarrow min(\sum_{t}(PO(t) * t * p_e - OPEX(t)) \geq CAPEX) \tag{2.1}$$

Advantages of using the payback period is that this metric is relatively easy to compute, and gives a clear idea of the profitability of a device at a certain location. If the PBP is small, this indicates a device that will earn itself back fast. If the PBP is larger than the lifetime of a device, the profitability is negative: such a device will only costs money. Disadvantages include that the PBP does not take the time-value of money into account, and the calculation 'stops' when the PBP is reached. Cash flows beyond that point are not taken into account.

2.3.2 Levelized Cost of Electricity (LCOE)

A way to take the time-value of money into account, and to consider all cash flows during the lifetime of a device, is by considering the Levelized cost of Electricity (LCOE). The LCOE is the ratio of the sum of all discounted cost flows and the discounted power output over the lifetime of the devices, and the most general form is given in Equation 2.2 (Blok and Nieuwlaar, 2016), in which $I(t)$ is the investment cost (that can happen any other time step than the first one, or on multiple ones, hence the denoted t), $M(t)$ the costs of maintenance, $F(t)$ the cost of fuel, r the discount rate, and $E(t)$ the energy output per time step.

$$LCOE = \frac{\sum(\frac{(I(t)+M(t)+F(t)}{(1+r)^t})}{\sum \frac{E(t)}{(1+r)^t}} \tag{2.2}$$

In the case of a single WEC, the investment is done in the first time step, and all costs related to the operational phase of the device are summarized in the OPEX, so Equation 2.2 can be simplified to Equation 2.3

$$LCOE = \frac{CAPEX + \sum(\frac{(OPEX}{(1+r)^t})}{\sum \frac{E(t)}{(1+r)^t}} \tag{2.3}$$

Interpreting the LCOE is simple: projects with a low LCOE are favourable over projects with a high LCOE. One can add any externalities in the calculation of the LCOE, as long as they are expressed in monetary terms. However, more abstract terms, like the degree of variability, are not taken into account in the LCOE. Previous studies have shown that wave energy has in general a higher LCOE over offshore wind, but a main advantage of wave energy, the lower variability and therefore a reduced pressure on the energy system, is not taken into account in the LCOE.

2.3.3 Value Adjusted Levelized Cost of Electricity (VALCOE)

There are metrics that include an attempt of taking variability into account. One of those, developed by the IEA (IEA, 2018), is the Value Adjusted Levelized Cost of Electricity (VALCOE). The VALCOE, taken from Graham (2018), is presented in Equation 2.4.

$$VALCOE_x = LCOE_x + (\bar{E} - E_x) + (\bar{C} - C_x) + (\bar{F} - F_x) \tag{2.4}$$

As can be seen in Equation 2.4, the VALCOE is the LCOE with three added terms. These three new terms, which are discussed in detail in the next sections, deal with the costs or revenues related to the integration of an energy technology, referred to as 'technology X', into the energy system.

The first added term, the second term on the RHS, is referred to as the 'Energy Adjustment' and represents the difference in revenue of the system (E_x) and the average revenue (e.g. the average electricity price) of the total energy system the technology X is embedded in ($\bar{E}$). This term therefore takes revenue into account, whereas the LCOE only deals with costs. Sometimes, the Energy Adjustment is referred to as the Value Adjustment. The second added term, the third term on the RHS, is referred to as the 'Capacity Adjustment', and deals with the increased or decreased adequacy to meet extra load as a consequence of the integration of technology X. Adequacy is defined as the ability of an energy system to meet the load at any time. Adequacy is becoming of greater importance with the integration of more variable renewable energy sources into the energy system (see for example Welsch et al. (2015)). The third added term, and the fourth term on the RHS of Equation 2.4, is referred to as the 'Flexibility adjustment', which is the difference in flexibility, put into monetary terms, between the technology X and the energy system.

According to IEA (2019), a key advantage of the VALCOE is that it is a more sophisticated metric that takes into account more properties of the system and the technology. However, environmental externalities, network integration and fuel diversity are not taken into account, and when using this approach, one adds more parameters and therefore more uncertainty into the calculations. The value of the VALCOE does not represent the real costs a market party has to pay, but rather a weighted summation of different properties of technology X and the energy system combined, expressed in the same monetary unit. The VALCOE is therefore more interesting for national grid operators, scientists and governments, whereas the LCOE is more relevant for investors.

2.3.3.1 Energy Adjustment

The Energy Adjustment, or Value Adjustment, term can be calculated, adapted from IEA (2019), according to Equation 2.5, in which P_o is the power output (often in MWh) of the technology during a time interval, p_e the electricity price during the same time interval.

$$E_x = \frac{\sum_h^{8760}(p_e * P_o)}{\sum_h^{8760} P_o} \tag{2.5}$$

In this research, time series of electricity prices of both locations were used, and were combined with timeseries of the sea state and the power matrices to compute the hourly revenue for each WEC. Then, this value was divided by the total power output over that time, which gave the Energy Adjustment of the WECs. Then, as benchmark and as average energy value $\bar{E}$, the average electricity price of the location is used. Those two terms subtracted from each other give the second term on the RHS of Equation 2.4. Suppose wave energy is more dominant during peak load hours when the electricity price is high, the energy value computed by Equation 2.5 is likely higher than the average electricity price and therefore a negative adjustment to the LCOE, vice versa if wave energy is producing more power during off-peak hours.

2.3.3.2 Capacity Adjustment

The Capacity Adjustment can be calculated using Equation 2.6, again adapted from IEA, 2019. In Equation 2.6, C_{cx} is the Capacity credit of technology X, which is explainable as the 'adequacy to meet a new load' of a technology. Its value is 1 if technology X will never have unplanned outages and one can increase the load with exactly the rated capacity of the technology. Taking planned and unplanned outages, and variability into account, makes it practically impossible for this value to be 1. B_{cv} is the basic capacity value set by the capacity market (often in \$/kW). C_{fx} is the capacity factor, which is the ratio of average power production over rated peak power of technology X.

$$C_x = \frac{C_{cx} * B_{cv}}{C_{fx}} \tag{2.6}$$

The adequacy of an energy system or technology is often expressed in the Loss Of Load Probability (LOLP), which is the chance that at any moment the load of a system cannot be met with the generators present. In other terms, all power plants together fail to meet the load that the total energy system requires, and (some) actors will receive less power than required. One could argue that a minimum requirement for system expansion therefore would be to keep the LOLP at least constant, or preferably decrease it.

To determine if the LOLP will not increase when adding load or generators to an energy system, one can rely on nationwide energy system models with high time resolutions in which for example an extra generator can be added. The model will then be run again with the extra utility, and the LOLP can be computed through multiple iterations. Adding a new generator into the system will most likely decrease the LOLP, since there is more power to be generated. Then, one can increase the load in the system until the LOLP from before adding the extra generator is reached. Dividing the extra load by the rated power of the generator will give the amount of power the load can increase per amount of power added to the system by the generator, which is the capacity credit.

These calculations are computationally intensive and require access to an elaborate energy system model, which lies beyond the scope of this research. There are methods of approximating the C_{cx}, for example shown in Keane et al. (2010) or Frew (2017).

One of the methods of approximating C_{cx} is the Z-method, developed by Dragoon and Dvortsov (2006). Dragoon and Dvortsov (2006) mathematically derived an approximate requirement that has to be fulfilled if load and generation increases in an energy system, to avoid the LOLP from increasing. This calculation is based on the surplus during peak hours, system reliability and the variance in power output of the added generator. Keane et al. (2010) compared the Z-method to the iterative model solution for adding more wind capacity to the energy system, and found that for low penetrations, the Z-method produces almost exactly the same results as the iterative solution obtained by using sophisticated energy system models. Keane et al. (2010) also explicitly mention wave energy as one of the technologies suitable to apply the Z-method on.

The Z-method, or similar methods including the computationally expensive energy system models, have been used by national grid developers to assess the adequacy of their future energy system. Great Britain uses the LOLP as main metric of system adequacy (Söder et al., 2020), which is also the key of the Z-method. The European Union explicitly recommends using probabilistic methods, such as the Z-method or the computationally expensive energy system models, over deterministic methods to calculate future system adequacy (Mercados, 2016).

The surplus of a system is the difference between resource availability and load at peak load

hours, given in Equation 2.7, in which R_t is the available generation at time t and L_t the total load on a system at time t. If the surplus is below zero, it is referred to as 'deficit'.

$$S_t = R_t - L_t \tag{2.7}$$

If there is enough (model-)data available, one can construct a probability density function of the surplus available. The approach of Dragoon and Dvortsov (2006) is then to recognize the surplus to be a probabilistic parameter and to construct a parameter, Z, that quantifies the adequacy of a system to meet its peak loads. The equation for Z is presented in Equation 2.8, in which $\overline{S}$ is the mean surplus and σ_s the standard deviation of the surplus.

$$Z = \frac{\overline{S}}{\sigma_s} \tag{2.8}$$

Systems with a high Z-value will be more reliable because either the mean surplus $\overline{S}$ is far away from zero, or the standard deviation σ_s is low. Both make the probability of a surplus below zero very low. A graph, showing the relations between the given parameters, taken from Dragoon and Dvortsov (2006), is presented in Figure 2.1.

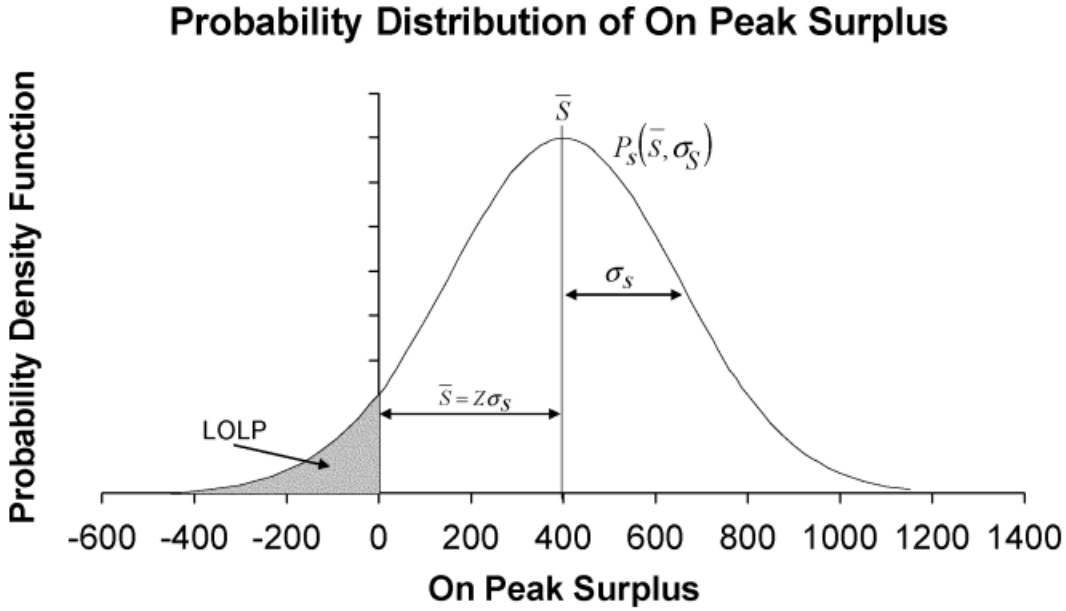

Figure 2.1: *Probability density function of an example surplus, taken from Dragoon and Dvortsov (2006). $\overline{S}$ represents the most likely surplus to find, in this case 400 MW. The surplus can become below zero, highlighted by the grey area. The area below the graph below zero divided by the total area is the LOLP.*

The requirement then derived, starting from the requirement that Z will not decrease when adding a new technology or generator ($dZ \geq 0$) is presented in Equation 2.9, in which R' is an increment in extra generation, Z_0 the Z-value (from Equation 2.8) before expansion, σ_s the standard deviation of the surplus before expansion, $\sigma_{L'}$ and $\sigma_{R'}$ are respectively the standard deviations of the load increment and the standard deviation of the new generator's output.

$$R' - \frac{Z_o}{2\sigma_s}(\sigma_{L'}^2 + \sigma_{R'}^2) \geq\approx L' \tag{2.9}$$

In words Equation 2.9 dictates that one cannot raise the load of a system by the same amount of MW as there is added by a new generator while keeping the same level of reliability, unless the standard deviation of both the load increase and generator increase is zero. This can only happen if it is absolutely certain what a new generator will produce, and how the load pattern of the energy system looks like in the future, and is therefore practically impossible.

In the case of this research, it is beyond the scope to predict the load increase, so it is more interesting to assess how much of the rated power of a generator, a WEC in this case, can increase the load of a system without increasing the LOLP. Dropping the load increment ($\sigma_{L'} = 0$), and rearranging Equation 2.9 gives Equation 2.10, in which P_i is the maximal fraction of the generators capacity that can be used to increase the load to keep the LOLP equal as before adding the generator (in MW/MW), therefore serving as a more elaborate capacity credit factor in Equation 2.6. The fraction is a function of the most probable surplus and it's standard deviation, which are properties of the energy system and therefore do not change between technologies. The fraction is furthermore quadratically dependent on the standard deviation of the generators output: generators with a more variable output and a larger standard deviation will have a (far) lower P_i compared to generators with low variability and therefore a lower standard deviation.

$$P_i = \frac{L'}{R'} = 1 - \frac{Z_0 \sigma_{R'}^2}{2\sigma_s R'} = 1 - \frac{\overline{S}_0 \sigma_{R'}^2}{2\sigma_s^2 R'} \tag{2.10}$$

However, the R' installed capacity is defined by Dragoon and Dvortsov (2006) as the capacity after the deterministic failure rate, such as the forced outages, have been taken into account. R' is presented in Equation 2.11, in which f is the unavailability rate and I_c is the rated installed capacity. The unavailability rate is made up of the failure rate and the repair times. The failure rate is defined as the frequency of failures during the lifetime of the device, and the repair time is the time it takes to repair these failures. Combined in the unavailability rate, this gives the total fraction of time during the lifetime that the device is out of order due to failure and repair (Ericsson and Gregorson, 2018)

$$R' = (1 - f) I_c \tag{2.11}$$

Substituting Equation 2.11 into Equation 2.10, and rearranging gives Equation 2.12, which gives P_f, the fraction of the installed capacity one can increase the load with without decreasing the systems adequacy due to both increased variability of the energy system (second term on the RHS of Equation 2.12) and failure rates (third term on the RHS of Equation 2.12).

$$P_f = 1 - \left(\frac{\overline{S}_0 \sigma_{I_c}^2}{2\sigma_s^2 I_c} + f\right) \tag{2.12}$$

Note that by using the Z-method, it is assumed that the parameter Z remains constant when adding extra generators to the energy system, so it is assumed that the system's surplus and standard deviation of the surplus do not change. This is justifiable for small amounts of power integration, and likely the reason why the Z-method starts to deviate from elaborate energy system model calculations for larger integration, as proved by Keane et al. (2010).

To compute the capacity adjustment of the VALCOE and use it in combination with the LCOE, it is needed to give a monetary value to the capacity credit. The base capacity value combined with the result of Equation 2.10 gives a monetary value of the added capacity, while taking into account the load increase the new system can handle 'safely', without decreasing its adequacy. The capacity credit is determined differently per country. The UK holds auctions at which capacity is bought by the National Grid operator, results of those auctions, including the clearing prices, are published (GOV.uk, 2020). Sweden's transmissions system operator (TSO) Svenska

Kraftnät highlights that currently no single party is responsible for sufficient capacity, in practice the local grid operators are mainly concerned with adding or removing installed capacity (Svenska Kraftnät, 2017). This makes it harder to find a single value for the capacity credit in Sweden.

2.3.3.3 Flexibility adjustment

The Flexibility adjustment, adapted from IEA (2019) can be calculated according to Equation 2.13. In Equation 2.6, F_{vm} is the flexibility value multiplier, and is equivalent to C_{cx}: a fully flexible technology receives a value of 1. B_{fv} is referred to as the Base flexibility value, and is a function of the share of variable renewables in the energy system. If there are more variable renewables embedded in the system, this value increases, because an additional flexible technology can (partly) offset the increased variability.

$$F_x = \frac{F_{vm} * B_{fv}}{C_{fx}} \tag{2.13}$$

More information on the methodology to calculate the flexibility adjustment is not provided by IEA (2019). In fact, a similar methodology to calculate the flexibility adjustment as was found for the capacity adjustment seems to not exist. Therefore, it is decided to not include the flexibility adjustment into this research.

In this section the methodology is presented. First, the different data sources for WEC properties, the sea state and the power systems are discussed. Then, the way of analyzing this data is presented. This chapter is concluded with a summary of the Monte Carlo analysis to be conducted. All data analysis and model calculations were done in Python.

3.1 Data sources

There are four main data categories used for this research: 1) Power matrices of the WECs 2) economic data of the WECs 3) data on the wave climate and 4) data on the power system. Data sources 1), 2) and 3) together can be used to compute the power output time series, and therefore the revenue, PBP and LCOE of the WECs over their lifetime. Data source 4) is needed to assess the influence a WEC has on the power system to compute the Capacity Adjustment and the Value Adjustment from the VALCOE.

3.1.1 Power matrices

Power matrices are 2D arrays of the average power absorbed in different sea states, characterized by a significant wave height H_s and the peak period T_p. The significant wave height is the average height of the one-third highest waves, and its dimension is length (meters is often used as unit). The peak period is the period of the most energetic waves in the wave spectrum and its dimension is time (often measured in seconds). The power matrix summarizes for a certain WEC what it could produce in power (often kilowatt) for a given combination of H_s and T_p. An example of a power matrix, taken from Babarit et al. (2012), is shown in Figure 3.1. Power matrices differ per WEC, so some WEC-designs are more suitable in certain wave climates compared to others. Together with data on the sea state, the power matrices can be used to compute the total power output of a WEC.

Babarit et al. (2012) modelled the power matrix of eight different WECs by numerically solving the equation of motion that follow from the balance of forces working on the device. Seven of these power matrices are used in this study[1]. The WECs used and their abbreviations are summarized in Table 2.1 and or an extensive description and examples of the seven WECs used, the reader is referred to Babarit et al. (2012).

The numerical method used by Babarit et al. (2012) seems to be a solid method of calculating the power matrices, and it does not rely on potentially confidential information of producers of WEC systems. It remains however a numerical approximation, which is not confirmed nor discarded by the industry. Therefore, in this research, additional power matrices from different sources are used to compare to the ones from Babarit et al. (2012). Data from other additional power matrices was often only visually presented in a contour plot, so to use this data, it had to be copied by eye. Then, because the installed capacity differed with the ones published in Babarit et al. (2012), the power matrix was divided by the installed capacity to get a percentage of the maximum power output, instead of kW, as unit. Also, published power matrices had different resolutions compared with the ones published in Babarit et al. (2012), so for every additional matrix, the closest H_s and T_p combinations were found and compared with the ones

[1] one of the power matrices of Babarit et al. (2012) is of a device that is operative on the sea floor, which is beyond the scope of this work

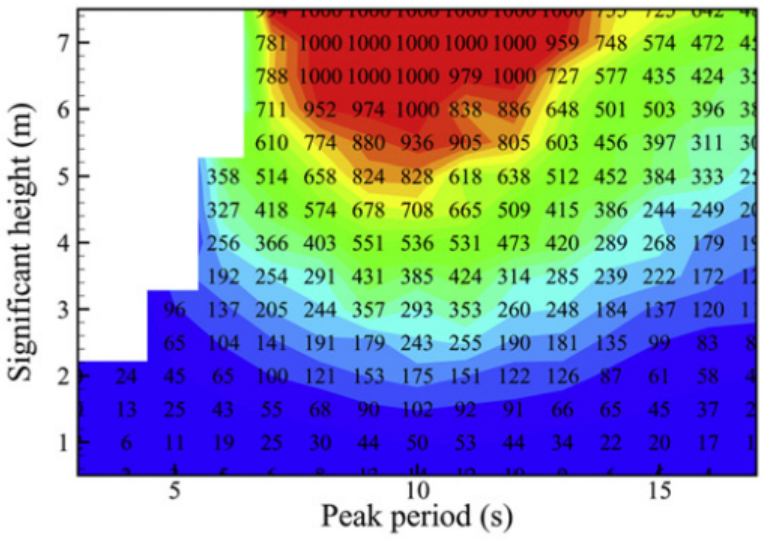

Figure 3.1: *Example of a power matrix of a floating two-body heaving converter (F-2HB) from Babarit et al. (2012). The numbers are in kW, the colours emphasize the power production of the device, and the white area highlights the combination of T_p and H_s for which the machine is not turned on, because it would either be unfeasible to let it run or dangerous for the construction.*

from Babarit et al. (2012). In this process, points are discarded from the analysis, because they fell out of the H_s and T_p range from Babarit et al. (2012). From the matching points, the Root-Mean Square Error (RMSE), R and mean bias were determined. The RMSE is calculated as follows: for all overlapping points in the two matrices the difference is taken. Then, the difference (or 'error') is squared. From this squared error, the mean is taken and square rooted. The RMSE gives a pure measure of the error between two data sets, eliminating positive and negative errors by squaring. The RMSE does not say anything about the sign of the error: if the power matrix of Babarit et al. (2012) predicts on average a larger power production compared to the ones in the literature. For this the mean bias is computed: which is the mean of the difference between the points of the two power matrices, without squaring. Both the mean bias and RMSE give information on the absolute value match, but nothing explicitly about the shape-match of the power matrices: for this Pearson correlation coefficient, R, is used. An R value close to one indicates a good match, and vice versa.

3.1.2 Economic data

Exact economic properties of WECs as given by the developers, are hard to find. Producers of WECs are hesitant in sharing this information because of its competitive value. There are multiple studies that use estimations, for example based on the IEA or estimates from The Association of Renewable Energy Producers (Astariz and Iglesias, 2015). Astariz and Iglesias (2015) give a comprehensive overview of the investments and the costs related to the operation of WECs. A comprehensive overview of costs of a theoretical Bref-HB WEC is presented by Ericsson and Gregorson (2018).

From the range of CAPEX and OPEX found in the literature, the ones computed by Oliveira-Pinto et al. (2019) are believed to be trustworthy, although being on the low end of the range, so these are the ones used in this research. Moreover, using the CAPEX and OPEX from Oliveira-Pinto et al. (2019) allow for an almost direct comparison and therefore verification of the LCOE

of this research with the ones computed by Oliveira-Pinto et al. (2019), as they use the same power matrices on a comparable location.

The CAPEX and OPEX from Ericsson and Gregorson (2018) are the highest ones found, almost six times higher than the ones computed by Oliveira-Pinto et al. (2019), and are therefore used as the upper limit in the Monte Carlo analysis of this study. Other studies that mention economic data for the WECs used in this paper, in the range between the CAPEX and OPEX computed by Oliveira-Pinto et al. (2019) and Ericsson and Gregorson (2018) and in addition to the studies listed in the introduction are the following: Chang et al. (2018a), Biyela and Cronje (2016), O'Connor et al. (2013) and , Previsic et al. (2012), De Andres et al. (2016).

3.1.3 Wave climate: WaveHub

Data on the sea state of the WaveHub site, is retrieved from a 23-year hindcast timeseries from Nieuwkoop et al. (2013), constructed using the wave model SWAN verified by buoy measurements. The location of the WaveHub measurement site is presented in Figure 3.2.

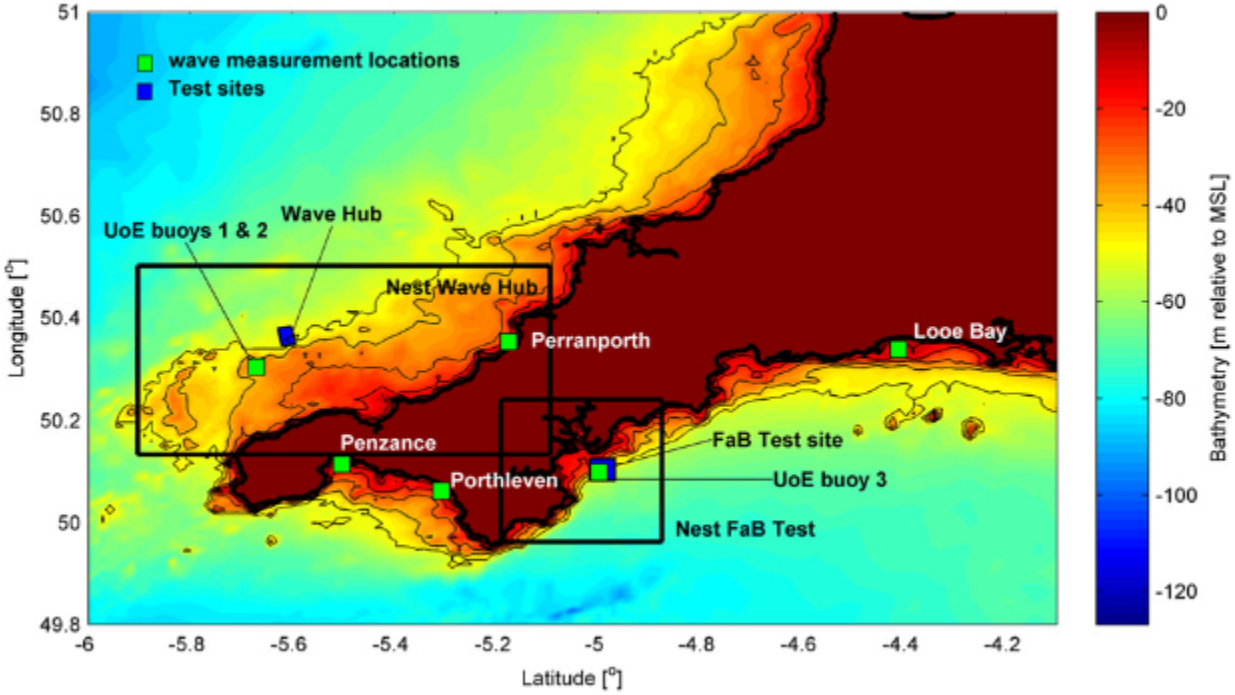

Figure 3.2: *Location of the WaveHub test site, and other measurement buoys, including bathymetry of the observed area, on the most south western point of the UK. Taken from Nieuwkoop et al. (2013).*

The data set provided by Nieuwkoop et al. (2013) consists of a timeseries of the significant wave height and energy period for the period 01-02-1990 to 01-11-2012, with hourly resolution. From this timeseries, a probability matrix was constructed by counting the occurrences of all H_s and T_p combinations. The probability matrix, in percent of the total data points, is presented in Figure 3.3.

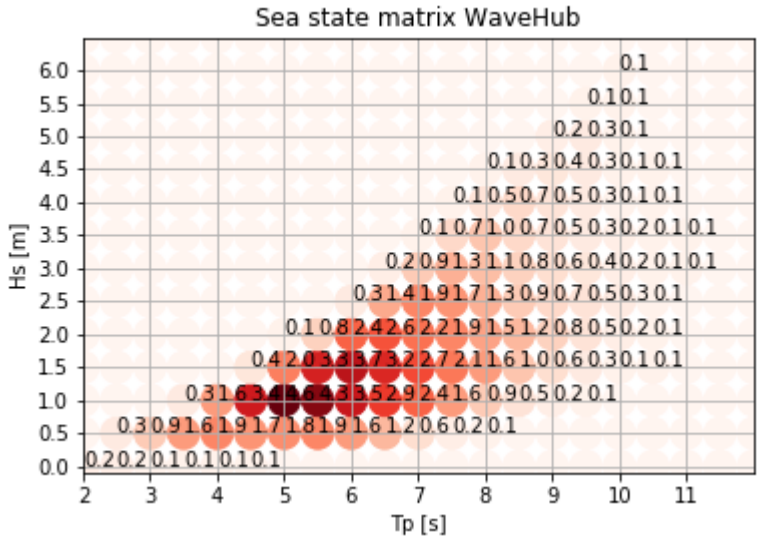

Figure 3.3: *Probability matrix constructed from the timeseries provided by Nieuwkoop et al. (2013). Numbers in the matrix are in percentage of the total occurrences.*

3.1.4 Wave climate: Lysekil

Data on the sea state of Lysekil is provided by dr. Malin Göteman, and first published in Waters et al. (2009). The location where the measurements were made is presented in Figure 3.4. The raw data consists of elevation measurements of the buoy around a reference sea state height of the years 2011-2017, with a frequency of 2.56 Hz. The data is collected in blocks of 30 minutes, each block containing 4608 measurements. These 30 minutes blocks are long enough to calculate the statistical parameters H_s and T_p, and short enough to elimate effects of the tides.

At first, the data is preprocessed, to estimate the quality of the 30 minutes blocks. That is, if the buoy was for any reason not able to measure the sea surface elevation, the data was discarded. If there are two faulty measurements happening close after each other, the whole sequence between them and the two data points at both ends of the sequence are taken out. The limit for labelling an error as 'close' to a previous error is arbitrarily set at 7 data points (roughly 3 seconds). An example of a refined half hour datablock can be observed in Figure 3.5. If a 30 minutes block of measurements contains too much unusable measurements (if after deletion the list becomes less than 500 items long), the 30 minutes block is regarded as unusable.

In the datasets 2011 - 2017, several months contained unusable data blocks. The missing data in these months are discarded, and averages of T_p and H_s of the months in other years are used. This will likely decrease the variability in the dataset, but is necessary to rule out seasonal biases. Alternatively, one could choose to exclude those months completely from further analysis, but then the sea state probability matrix will be more heavily determined by data from the Summer and Autumn, for which there are likely different wave conditions than Winter and Spring. Filling up gaps in months with averages of the same months therefore rules a seasonal bias out.

The dataset can then be used to calculate, per 30 minutes block, the significant wave height

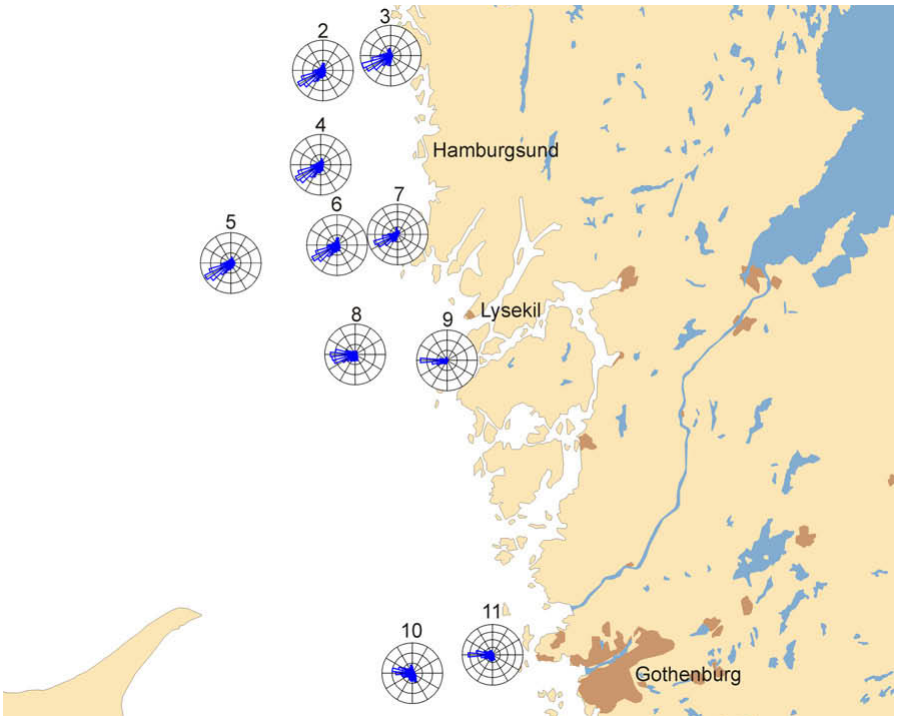

Figure 3.4: *Locations of the measurements made for the Uppsala University by Waters et al. (2009), image is also taken from Waters et al. (2009). Location 9 is where previous studies were done with WECs developed by the Uppsala University (see for example Lejerskog et al. (2015)), so this location is used in this research as well.*

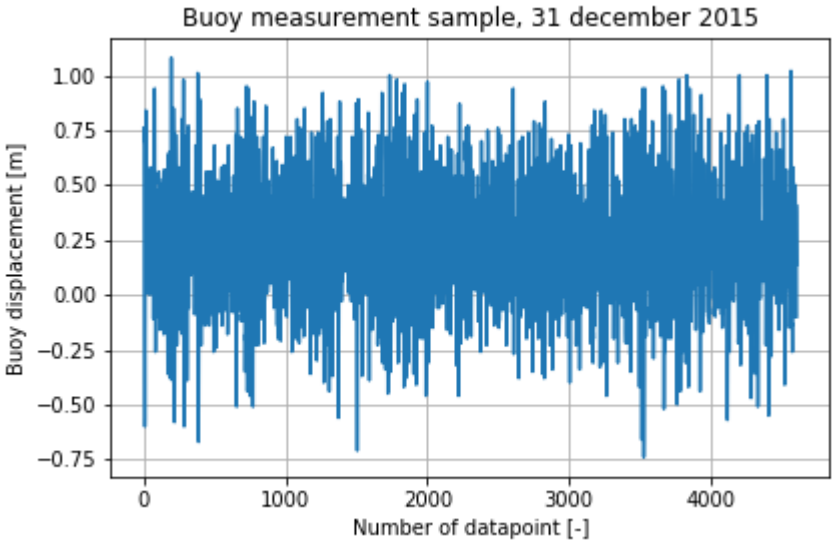

Figure 3.5: *Sample of buoy displacement data for the half hour chunk 23:30 - 0:00 at the 31st of December 2015.*

and peak period. The following steps are taken to obtain the significant wave height and the peak period. First, the Fourier coefficients are determined from the buoy displacement, such as the one in Figure 3.5, written out in Equation 3.1. In Equation 3.1, $x(n)$ is the n^{th} buoy measurement of a total of N measurements, and k the corresponding frequency. $x(k)$ is the Fourier transform.

$$x(k) = \sum_{n=0}^{N-1} x(n) \exp \frac{-i2\pi kn}{N} \tag{3.1}$$

Then, the spectral density of the Fourier transform is determined by taking the absolute value of the Fourier coefficients, by multiplying each Fourier component with its complex conjugate. The result is a list of the power of every Fourier component. The peak period Tp is defined as the period where the spectral density has its maximum. (6.14 seconds for the case of Figure 3.5). This is written out in Equation 3.2, in which the denominator makes the T_p in seconds.

$$T_p = \frac{max(2 * x(k) * conj(x(k))))}{30 * 60} \tag{3.2}$$

The significant wave height can be obtained by, per definition, multiplying the square root of the variance of the dataset by four. The variance, per definition the first spectral moment, is computed by integrating the power spectrum over the frequency domain. This is done using the trapezoidal approximation. The square root of the result, multiplied by four, gives the significant wave height H_s (1.14 meters for the case presented in Figure 3.5). The process is written out in Equations 3.3a and 3.3b, in which m_0 is the first spectral moment, also known as the variance. The infinite integral in equation 3.3a is approximated using the trapezoidal method.

$$m_0 = \int_{-\infty}^{\infty} x(k)\delta k \tag{3.3a}$$

$$H_s = 4 * \sqrt{m_0} \tag{3.3b}$$

The resulting timeseries of T_p and H_s were then in the final step processed in the same way as the data from Nieuwkoop et al. (2013), and the resulting sea state probability matrix is presented in Figure 3.6.

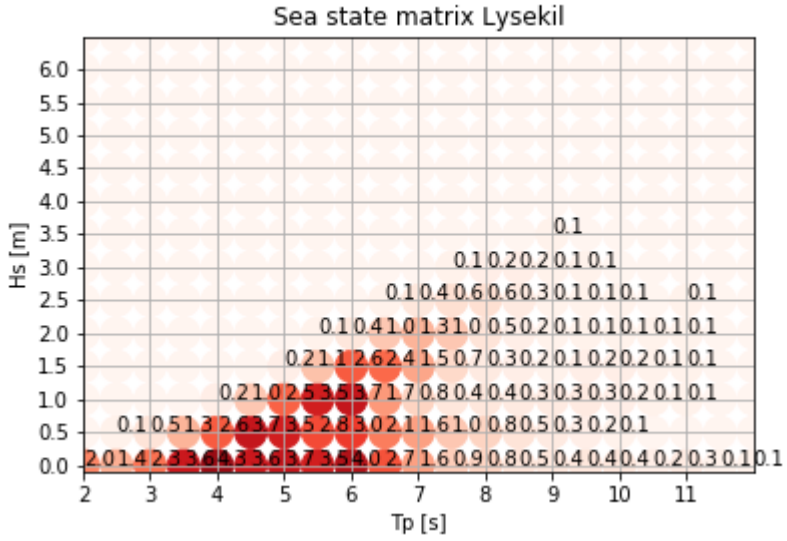

Figure 3.6: *Sea state probability matrix Lysekil, based on the years 2015-2018.*

Comparing the wave climate of Lysekil with the one constructed for the WaveHub site shows that the wave climate at WaveHub contains on average sea states with a higher T_p and H_s, which is often associated with a higher power output of a WEC, but also with a rougher sea, therefore higher failure rates and higher repair costs.

3.1.5 Power System Data

For the parts of the VALCOE used in this work, power system data is needed, such as total load, and total installed capacity. This data is available from the national grid operators and the national statistics offices. For Sweden, see SCB (2020) and Svenska Kraftnät (2020). For the UK, see National Grid (2020) and Office for National Statistics (2020). The European Network of Transmission System Operators for Electricity (ENTSO-E) Transparency database is a gathering of this data in one database, for a large number of European countries, for several variables and time scales. However, it proves to be time consuming to download all required data separately for larger time scales from the ENTSO-E database, and for this purpose the Open Power System Data platform (see OPSD (2020)) was developed, containing collections of timeseries obtained from the above mentioned sources. The 60 minute resolution data table contains for both locations (the UK and SE3, the Swedish power system region Lysekil is embedded in) time series of different sources (such as the National Grid and the ENTSO-E), all gathered in one large datafile. For the case study on Malta, the work of Bugeja (2020) is used as main source for power system data.

3.2 Data analysis and model construction

The data analysis and model calculations were done by refining and combining the before mentioned data sources. First, the sea state probability matrices and power matrices were combined to compute the Annual Energy Production (AEP) per device at both locations. Then, the AEP is combined with the economic data, and in some cases with power system data, to compute the PBP, LCOE and the relevant parts of the VALCOE. This process is simplified summarized in Figure 3.7.

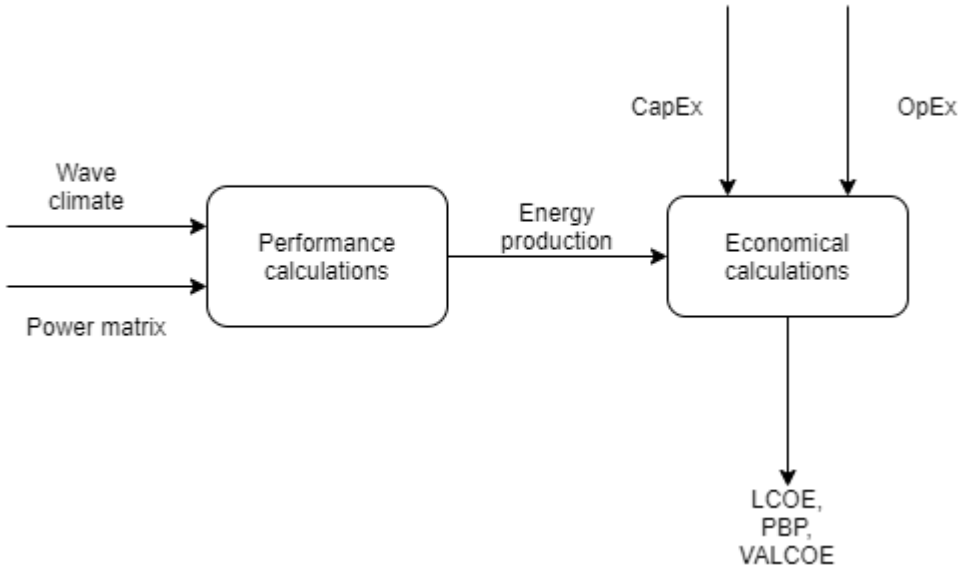

Figure 3.7: *Simplified version of the methods to be used. This process wil be repeated for every WEC and every location, so the final output consists of the LCOE, PBP and different VALCOE contributions of seven different WECs on two different locations.*

3.3 Data sources: Lifetime, failure rates, Feed-in Tariffs and base capacity values

The following two sections cover the additional sources of input data, starting with the economic calculations in this section and followed by the time series used in this research in the next section.

The lifetime of the devices is fixed at 20 years, following the range in the literature listed in section 3.1.2. The discount rate remains a source of uncertainty in renewable energy technology (Leskinen et al., 2020). Oliveira-Pinto et al. (2019) mention a range between 5%-15%, while using 10% in their research. Giassi et al. (2020a) did a similar review and assumed a discount rate of 8%. Castro-Santos et al. (2015) used three different discount rates, respectively 5%-7.5%-10%. Astariz and Iglesias (2016b) use three discount rates as well, but slightly higher: 6%-10%-15%. It is clear that the discount rates used before are mostly in the range 5%-15%, so in this research the approach of Oliveira-Pinto et al. (2019) is used by initially assuming the discount rate to be 10%.

Several countries have financial support schemes in place for renewable energy technologies. These support schemes can for example be a Feed-in Tariff (FIT), which is a price producers get per produced MWh, regardless of the Day-Ahead price. A Feed-in Premium can also be issued, which is a percentage on top of the Day-Ahead price, thereby making it dependent on electricity-demand.

In Sweden, a market-based cap-and-trade system is in place. The government sets targets for energy producing companies in the form of a certain percentage of the total energy production that has to come from renewable sources. For every MWh produced using renewable sources, companies get an electricity certificate. Companies that are not able to meet this obligation can

buy electricity certificates from companies that have a surplus of renewable energy certificates. See Energimyndigheten (2019) for a full explanation. The obligation in 2018 was 29.9%, and the average price of trading the electricity certificates was 154 SEK/certificate in 2018 (Swedish Energy Agency, 2019). Therefore, in this research, it is asummed that the electricity at Lysekil can be sold at the Day-Ahead price plus 70.1% for 154 SEK per MWh. Furthermore, Sweden has a carbon tax implemented, of 1190 SEK per kg CO_2 emitted in 2020 (Government Offices of Sweden, 2018). The average emission factor in Sweden was 0.0120 kgCO_2 per kWh (Footprint, 2019). Combining these metrics gives an average carbon tax of the Swedish Energy System of 14.48 SEK/MWh. This is not a net profit when using WECs, but it is an advantage over the average of the system and will only be used in calculation of the VALCOE Value Adjustment.

The UK has recently abolished any financial support renewable energy producers could get (see Ofgem (2020)). Although a FIT was in place before 2019, it cannot be assumed or estimated if and at what price it will come back. Therefore, in this research, initially there is no FIT, FIP or renewable subsidy available for the WECs deployed at the WaveHub site.

The base capacity value is determined from results of the capacity market in place in both countries. For the UK, the average resulting clearing price of the auctions held in 2015, 2016 and 2017 is used, which can be retrieved from GOV.uk (2019). For Sweden, results of the Nordic adequacy system are used, referred to as the FCR prices (Pihl, 2019). It has to be noted that the FCR system will in the near future be abolished in favour of the new ACE system (Svenska Kraftnät, 2018), but no data is yet available on the prices per kW to be used in the neW ACE system, so the FCR prices are used in this research.

Due to the difference in currencies: GBP for the UK, SEK for Sweden, EUR for Europe and the Open Power System Data, and USD for other studies to compare with, all currencies in the following calculations are done in USD.

3.4 Data sources: Time series

All four data categories contain time series, with different resolutions and ranges. This section summarizes how time series with different resolutions where processed before being used to compute the PBP, LCOE and the different contributions to the VALCOE.

Generally, the time series with the lowest range and resolution was used as benchmark-minimum quality input for the physical and economic calculations, and all other time series used in the same calculation steps were adjusted accordingly, and interpolated if needed. Interpolation happened in the following way: first, the time range for interpolation was determined. Then, an empty time-vector with the desired range and resolution was constructed. Finally, the time series that requires interpolation was linearly interpolated over the new time vector. A summary of all time series, their resolution, potential gaps, and their source are listed in the following sections.

3.4.1 Time series: sea state data

The sea state probability matrices (Figures 3.3 and 3.6) are based on the two time series discussed extensively in section 3.1.3 and 3.1.4. The resulting resolution, range, source and the presence of gaps are summarized in Table 3.1.
In combination with the power matrices, these sea state time series can be turned into a time series showing per interval the power production of every device in kW. The resulting power production time series have the same resolution as the corresponding sea state data of WaveHub.

Table 3.1: *Summary of sea state time series.*

Name	Range	Resolution	Gaps	Source
Hs, Tp Lysekil	01/01/2011 - 31/12/2017	Every 30 minutes	Yes	dr. Malin Göteman
Hs, Tp WaveHub	01/02/1990- 01/11/2012	Every 60 minutes	No	Nieuwkoop et al. (2013)

The sea state time series of Lysekil, having a 30 minute resolution, are downgraded to 60 minute resolution if needed, by interpolating them on an empty 60 minute resolution time vector of the desired range.

3.4.2 Time series: Pay Back Period

The CAPEX and OPEX are not time and/or location dependent in this research, but the revenue of every device is. The timeseries of power production, with the same resolution and range of the time series summarized in Table 3.1 are combined with timeseries on the electricity price to obtain per time interval the revenue of a WEC. The electricity price time series that were used in addition to the time series in Table 3.1 are summarized in Table 3.2.

Table 3.2: *Summary of the additional time series used for the PBP calculation.*

Name	Range	Resolution	Gaps	Source
Day-Ahead price UK	19/12/2014 - 30/04/2019	Every 60 minutes	Yes	OPSD (2020), National Grid (2020)
Day-Ahead price SE3	01/11/2011- 30/04/2019	Every 60 minutes	Yes	OPSD (2020), Svenska Kraftnät (2020)

The sea state of Lysekil is interpolated over a time vector with the same range but with a 60 minutes resolution, to fit with the Day-Ahead price time series. The overlapping years, 2011 - 2017, are used to create the revenue time series. The same procedure is used for WaveHub, the years 2007-2012 of the sea state time series are combined with the years 2014 - 2019 in the Day-Ahead time series. The corresponding revenue time series for Lysekil and WaveHub are respectively copied 4 and 5 times. The copies are then concatenated, to generate revenue time series that would have a large enough extent to overtake the (predicted) lifetime of the devices, since the extent of the original Day-Ahead price time series are 5 and 8 years, and the predicted lifetime is 20 years. It is thereby assumed in this research that these chunks of 5 and 8 years represent the electricity prices in the countries for 20 years.

It can be reasonably expected that the future Day-Ahead prices will be lower compared to the ones from the time series used, because of the larger scale integration of wind power generation. Therefore, when making future predictions, a potentially larger PBP should be taken into account.

3.4.3 Time series: VALCOE Value Adjustment

The timeseries used for the Value Adjustment are similar to the ones used for the PBP, but in this case they did not need to be repeated 4 or 5 times, since the value adjustment is an average value and repeating the time series does not change it. The regular Day-Ahead prices and time series of power production on both locations for all devices are combined. For the system average value adjustment, the average Day Ahead prices of both locations are used.

3.4.4 Time series: VALCOE Capacity Adjustment

The capacity adjustmtent of the VALCOE, more specifically the Z-method, requires the surplus in the energy system as input. The surplus in the energy system is defined by Dragoon and Dvortsov (2006) as the difference in installed capacity and load during the peak hours. To create a probability density function, the time series summarized in Table 3.3 are required. The installed capacity time series have an annual resolution. These time series are linearly interpolated to a step-wise monthly resolution, in which every month of a year the installed capacity is increased with $\frac{1}{12}$ times the total annual increase. In reality, the installed capacity will show a more irregular step-wise function throughout the year, a step corresponds to every time step a power plant opens or closes, but data is lacking to incorporate that.

To determine the peak load and surplus during peak hours, one has to define at what times peak load happens. There are multiple definitions for peak hours used in the literature. Brännlund and Vesterberg (2018) for example define peak hours between 4 and 9 PM as peak hours, whereas Vesterberg (2016) defines two peaks a day: one between 6 and 8 AM and one between 5 and 10 PM. Broberg et al. (2017) then defines peak hours from the demand curves of Sweden to be between 7 and 8 PM. One could also argue that peak hours should be determined from the load curves themselves, by for example defining peak hours as hours with 1 standard deviation above the mean load.

All things considered, for both countries, the definition proposed by Blanco et al. (2016) is used: On weekdays, between December and February, between 7:00 and 19:00, on days where the peak demand exceeds the 50th percentile of the total demand. This seems to be the most specific and comprehensive definition of peak hours found, which includes the assumption that demand is higher during Winter.

Table 3.3: *Summary time series used as input for the capacity adjustment.*

Name	**Range**	**Resolution**	**Gaps**	**Source**
Load UK	31/03/2005 - 30/04/2019	Every 60 minutes	Yes	OPSD (2020), National Grid (2020)
Load SE	13/12/2014- 30/04/2019	Every 60 minutes	Yes	OPSD (2020), Nordpool (2020)
Installed capacity UK	1892-2019	Every year	No	GOV.UK (2020)
Installed capacity SE	1996 - 2018	Every year	No	Energimyndigheten (2019)

The total installed capacity of Sweden could not be separated to their Energy Region (Lysekil is situated in region SE 3), so it is assumed that surplus of the energy system of the whole country

can be used as surplus for region SE 3 as well. Regions could deviate from the national average installed capacity. For example, the Swedish region SE 1 is situated in the North, where there is more heavy industry and a colder climate compared to the South, but SE 1 has also a smaller population. No literature was found to quantify these claims.

The installed capacity UK time series has a large range, and only the years needed in combination with the load time series of the UK are used.

3.5 Additional case studies

Two scenarios were developed to test the model, in addition to the four metrics calculated (PBP, LCOE, VALCOE-Value adjustment, VALCOE-Capacity adjustment) for the UK and Sweden. The first scenario is that of a park of several Bref-HB WECs at the Lysekil-site. Installing a park instead of one device will lower the CAPEX and OPEX, but also the power production due to hydrodynamic interactions, and the variability of the output. Values found in Ericsson and Gregorson (2018) and Göteman et al. (2014) are used to calculate the new set of parameters. The second scenario is related to the capacity adjustment. Sweden and the UK both have power systems deployed with massive amounts of surplus. In other words, these countries are extremely eager to avoid Loss of Load Days (LOLDs), and adding one WEC device has little effect on the systems adequacy. A smaller power system, of a remote small island for example, will give more interesting results. Remote small islands are more interesting for WEC development for obvious reasons. At the same time, they often have a smaller energy system and are therefore likely more affected by the addition of extra variable generators. Malta is used as a case study because power system data was available from Bugeja (2020).

3.6 Monte Carlo analysis

Given the large spread and uncertainty in multiple sources of the input data, it is chosen in this research to conduct a Monte Carlo analysis, rather than for example a linear sensitivity analysis. In a Monte Carlo analysis, one can change multiple input parameters at once and independently, which makes it possible to combine the uncertainties of different sources into one output uncertainty.

The Monte Carlo analysis is done by replacing the three most important input parameters: the power matrices, the CAPEX and the OPEX, with probability density functions (PDFs). The method of turning the power matrices into PDFs is dependent on the results of the power matrix comparisons, and will be further elaborated on in Chapter 5.

The shape and extent of these probability density functions is determined based on the spread of values found in the literature. Then, the model was run 1800 times to make sure enough sample points are present. The results are presented as 95% confidence intervals.

4 Results: Base cases

In this chapter, the results are presented. First, the results of the power matrix comparison are discussed. Then, the general outcomes of the techno-economic analysis are presented. Then, the PBP per device for both locations is shown, followed by the LCOE. Then, the Value Adjustment and Capacity adjustment are presented. This chapter ends with the results from both case studies.

4.1 Power matrix comparison

The results of the comparison of the power matrices published by Babarit et al. (2012) and other sources are summarized in Table 4.1.

Table 4.1: *Comparison of thirteen additional power matrices with the ones published in Babarit et al. (2012). Similar/same indicates that the additional power matrix is of exactly the same WEC assessed by Babarit et al. (2012) (same), or of a different system using the same technology (similar). Quality of the copy indicates how easily the data could be copied. 'Low' indicates a copy by eye of a coarse resolution contour plot with little axis indicators, 'literal data' means that the data from the power matrix could be downloaded directly. Number of points indicates the amount of points that could be compared. The power matrices from Babarit et al. (2012) contain 225 T_p and H_s combinations, which is therefore the maximum amount of points that could be used for the analysis.*

Name	**Similar/ same device**	**Quality of copy**	**Number of points**	**RMSE**	**R**	**Bias**	**Source**
-	*probably similar, similar, exactly the same*	*low, medium, numerical copy, literal data*	*max: 225*	*percent point*	-	*percent point*	-
Bref HB	similar	numerical copy	91	0,34	0,94	-0,29	Mérigaud and Ringwood (2018)
Bref HB	similar	medium	84	0,24	0,72	-0,04	Oliveira-Pinto et al. (2020)
Bref HB	probably similar	medium	49	0,37	0,53	-0,19	Ulazia et al. (2017)
Bref HB	probably similar	literal data	150	0,21	0,79	-0,14	Teillant et al. (2012)
Bref SHB	exactly the same	medium	84	0,26	0,30	-0,03	Oliveira-Pinto et al. (2020)
F3OF	exactly the same	medium	154	0,31	0,035	-0,07	Lavelle and Kofoed (2011)
F3OF	similar	numerical copy	91	0,34	0,65	-0,24	Mérigaud and Ringwood (2018)
F3OF	exactly the same	medium	84	0,24	0,44	-0,07	Oliveira-Pinto et al. (2020)
FHBA	similar	literal data	165	0,28	0,80	-0,16	Dalton et al. (2010)
FHBA	similar	literal data	72	0,23	0,90	-0,15	Diaz-Santamaria et al. (2014)
FOWC	probably similar	low	21	0,42	0,38	-0,26	Pecher (2012)
FOWC	similar	literal data	72	0,31	0,88	-0,18	Diaz-Santamaria et al. (2014)
FOWC	similar	numerical copy	150	0,29	0,86	-0,21	Sheng (2019a)

Pearson's R value (or correlation coefficient) is used in this study as the primary indicator of similarity: for some power matrices, including the ones from Babarit et al. (2012), it was not mentioned what the installed capacity was. In those cases, the maximum power output listed in the power matrix was chosen as installed capacity, and the rest of the power matrix is scaled to that value. This uncertainty causes the numerical values of the percentages in

the power matrices to be slightly uncertain, so the RMSE and mean bias, defined as the mean of the difference between all points of the two power matrices, might be off. The R value tells something about the shape match of the power matrix, which is less dependent on the exact numeric values.

In general the correlation coefficient R shows a good match between additional power matrices with a higher quality of copy compared to the lower quality copies. This leads to the conclusion that shape-wise the power matrices of Babarit et al. (2012) match pretty well with additional ones published. The RMSE is however quite high and the prevalent negative bias is striking. This means that the power matrices published by Babarit et al. (2012) are structurally reporting lower power production values compared to other power matrices found in the literature. This might be because the year of publication: All additional power matrices with the exemption of the F3OF by Lavelle and Kofoed (2011) are published more recently, while potentially the technology and therefore efficiencies have increased. The power matrices from Babarit et al. (2012) are still being used in this research, but the Monte Carlo analysis includes tests with scaled matrices to the mean bias, by using a multiplication factor, to get more insights in the effects of increased efficiencies. This is elaborated further on in chapter 6.

4.2 Techno-economic analysis

The used CAPEX and OPEX are summarized in Table 4.2. This study assumes that the CAPEX and OPEX are the same for both sites. In reality, a more energetic wave climate would likely imply both higher CAPEX (higher design loads demand more robust structures and more costly installation), and higher OPEX (higher failure rates, downtime, and repair costs). The Annual Energy Production and capacity factor per device for both locations are shown in Table 4.3. The revenue of all devices for both locations can be seen in Figures 4.1 and 4.2. The time series of the power production of the Bref-HB device at Lysekil and WaveHub is presented in Figure 4.3 to get an idea of what the power production time series look like.
When comparing Figures 4.1 and 4.2, two things should be noted. First, the total revenue for all WECs at the end of the lifetime is higher (around three times) at the WaveHub site compared to the Lysekil site, as a consequence of the higher AEPs. This is not unexpected: when comparing the sea state probability matrices (see Figures 3.3 and 3.6), one can observe that combinations of higher H_s and T_p, which are associated with more energetic seas and therefore likely cause a higher power production of WECs, are more abundant in the WaveHub site compared to Lysekil.

Table 4.2: *CAPEX and OPEX used, from Oliveira-Pinto et al. (2019).*

Name	**CAPEX**	**OPEX**
-	*EUR/kW*	*EUR/kW*
BHBA	4500	22.5
BREFHB	3312	331
BREFSHB	937	94
F2HB	1137	114
F3OF	610	61
FHBA	558	59
FOWC	1116	112

Table 4.3: *Annual Energy Production and Capacity factors for the seven WECs for two locations.*

	Rated Capacity (kW)	AEP Lysekil (MWh)	Capacity factor Lysekil	AEP WaveHub (MWh)	Capacity factor Wavehub
BHBA	2700	559	0.02	2222	0.09
BrefHB	15	7.7	0.06	23.6	0.18
BrefSHB	260	61	0.03	217	0.10
F2HB	1000	179	0.02	915	0.10
F3OF	1665	300	0.02	1088	0.07
FHBA	3619	1046	0.03	2740	0.09
FOWC	2880	191	0.01	1128	0.04

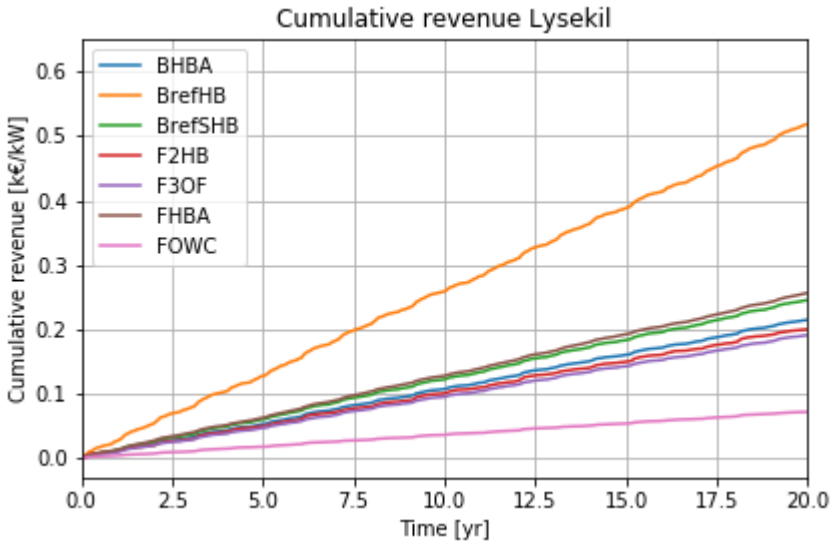

Figure 4.1: *Cumulative revenue computed for all WECs at the Lysekil site.*

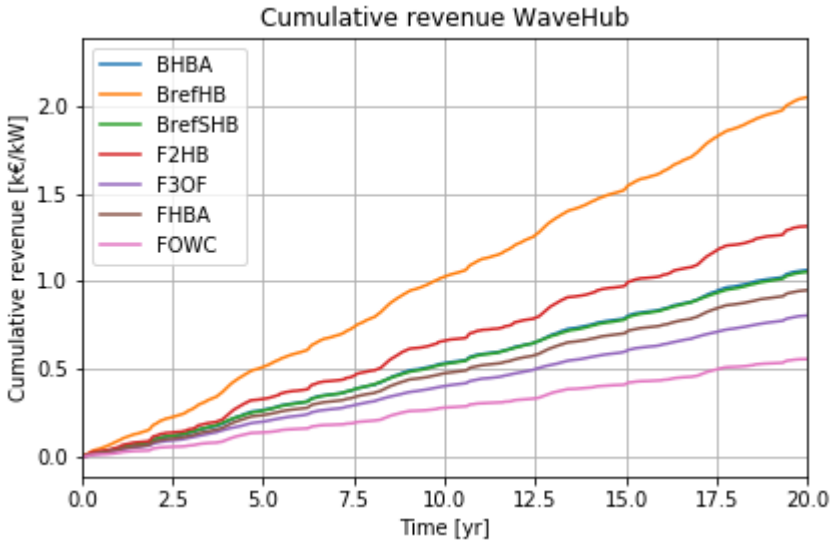

Figure 4.2: *Cumulative revenue computed for all WECs at the WaveHub site.*

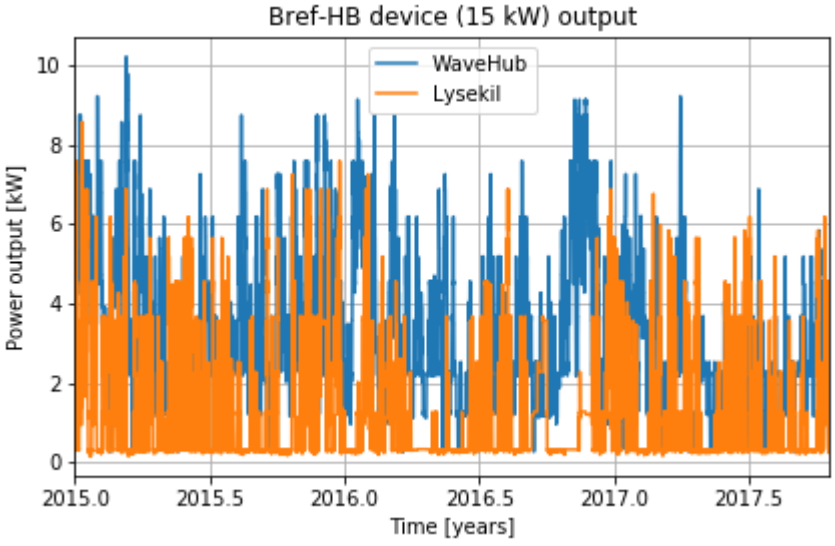

Figure 4.3: *Power production of the Bref-HB device deployed at both locations.*

Secondly, the order of devices from 'most revenue' to 'least revenue' is slightly different. For the WaveHub site, the relative difference in revenue between the FHBA and BHBA system is smaller than in Lysekil. Furthermore, the order of the systems FOWC, F2HB and FHBA is mixed between both sites, which is likely because some WECs are more suitable to certain sea states compared to others.

4.2.1 Pay Back Period

The PBP of all devices on both locations can be observed in Table 4.4. Table 4.4 shows the PBPs of all devices deployed at the WaveHub site are lower, compared to the PBP's of Lysekil, emphasizing again the larger potential of the WaveHub site. From this study it can be concluded that, for a single WEC (i.e. no cost savings present in a park, see chapter 4.8 for an example) whose average power is given by the power matrices in Babarit et al. (2012) (i.e. no control algorithms or other methods to enhance the energy absorption), a lifetime of 20 years is not sufficient to obtain a positive net revenue at the Lysekil site.

Again, it is clear that different WEC designs, with different power matrices, favour different wave climates. For example, consider the PBP of the Bref-SHB and the F2HB system. The F2HB preforms worse than the Bref-SHB at Lysekil. However, the F2HB preforms slightly better at WaveHub, compared to the Bref-SHB system, reflected by the slightly lower PBP. Also, for the FOWC system, the difference between locations is significant, with the WaveHub having an almost eight-fold higher percentage of the CAPEX covered, compared to around four-five fold for other devices.

Table 4.4: *The resulting Pay Back Periods. When the PBP was not reached in the lifetime of the WEC (20 years), the percentage of the CAPEX covered by the net revenues during this time is used to predict the PBP, since the timeseries used end after 20 years. If the PBP is below the lifetime of the device, the PBP in years is shown (green).*

Name WEC	**PBP Lysekil**	**PBP WaveHub**
-	*years*	*years*
BHBA	416.7	84.4
BrefHB	128.2	32.4
BrefSHB	76.3	17.5
F2HB	113.6	17.2
F3OF	63.9	15.1
FHBA	45.9	12.6
FOWC	312.5	39.9

Note that the 'most profitable' devices from Figure 4.1 and 4.2 are not the devices that have the lowest PBP, or the highest percentage of the CAPEX covered. The Bref-HB has the highest revenue for both locations per kW installed, but also by far the highest CAPEX of all devices considered. One could therefore expect that this device will profit the most from a CAPEX decrease because of technological learning, or when installed in a park to share structural elements with other devices and thereby lower the investments. More on the latter in section 4.8.

4.2.2 Minimal Feed-in Tariffs

The FITs present, being zero in the UK and 109.34 SEK per MWh in Sweden, are not sufficient to get all PBP's of the devices below the lifetime. It is therefore interesting to see what FIT would be required to make the WECs in terms of the PBP economically feasible. In order to assess this, the following method is used: for both location and all devices, the FIT is set to zero. Then, the PBP was calculated. If the PBP was larger than the lifetime, a new FIT of 10 $ per MWh more is tried, until the PBP goes below the lifetime. The first FIT where this happens is accepted as the minimal FIT for which the PBP goes below the lifetime. The results are presented in Table 4.5.

Table 4.5: *The FITs that need to be minimally implemented to get the pay-back periods below the lifetime, 20 years, of the devices.*

Devices	**Lysekil**	**WaveHub**
-	*min FIT ($/MWh)*	*min FIT ($/MWh)*
BHBA	830	150
Bref-HB	260	40
Bref-SHB	150	0
F2HB	230	0
F3OF	120	0
FHBA	80	0
FOWC	660	60
Average	333	36

The range of FITs to make the PBP below the lifetime is within the range of FITs present around the globe, see for example the database of the OECD (2019).

4.2.3 Levelized Cost of Electricity

The calculated LCOEs for all devices, on both locations, are summarized in Figure 4.4. Additionally, the LCOEs calculated by Oliveira-Pinto et al. (2019) are plotted as well. Again, when looking at the results in Table 4.4, but also when considering them together with the results presented in 3.2, one must keep in mind that a lower LCOE would probably be achieved at both sites if parks instead of a single WEC was installed (see the case study described in section 4.8), and that in reality the CAPEX and OPEX might differ at both sites leading to a less difference in the LCOE between both sites.

First, the LCOEs at Lysekil is orders of magnitude higher compared to the LCOE at WaveHub and the ones calculated by Oliveira-Pinto et al. (2019). This is certainly caused by the calmer wave climate at Lysekil (compare Figures 3.6 and 3.3). Especially the BHBA and FOWC device, whose power matrices from Babarit et al. (2012) are extremely favourable for high T_p and H_s combination. The FHBA and F3OF have a much more concentrated 'peak spot', an area of the power matrix where (almost) maximum power output is achieved. The LCOE seems to differ less for these devices.

The LCOE computed by Oliveira-Pinto et al. (2019) is in between the calculated LCOEs of WaveHub and Lysekil, for every device larger than the LCOE at WaveHub and smaller than the LCOE at Lysekil. Since the same CAPEX and OPEX are used, this verifies the calculations made in

this research. Differences are likely caused by three differences between the approaches of this research and Oliveira-Pinto et al. (2019): 1) Oliveira-Pinto et al. (2019) made use of an inflation rate, which will make the LCOE higher compared to the ones calculated in this research, 2) In the calculations of Oliveira-Pinto et al. (2019), three failure rates related to mechanical, power conversion and device efficiency are considered, which together account for roughly 20 % less power production per device, making the LCOE computed by Oliveira-Pinto et al. (2019) likely higher and 3) Oliveira-Pinto et al. (2019) use sea states obtained further off the Norwegian coast, as their research is about the potential to couple WECs to offshore (oil) platforms. This research uses near-coast power matrices, where on average the wave climate is expected to be calmer.

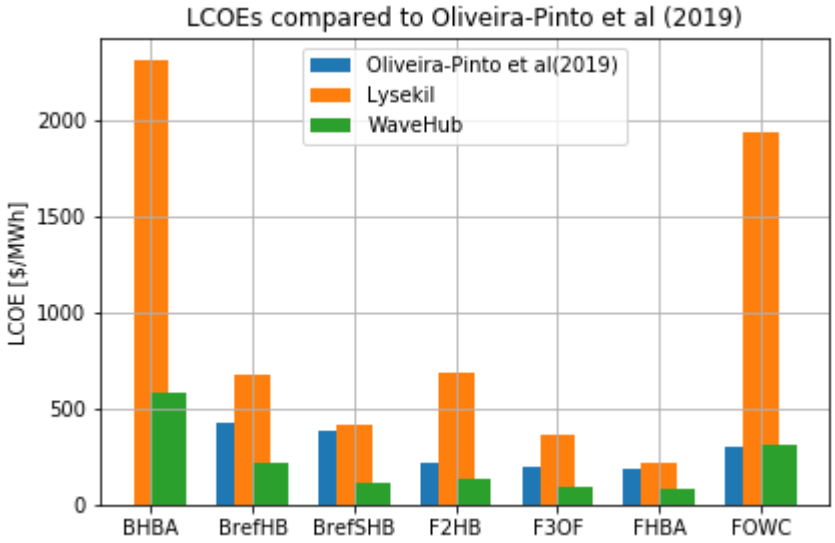

Figure 4.4: *Levelized Cost of Electricity for all devices at Lysekil, WaveHub and computed by Oliveira-Pinto et al. (2019). The BHBA device was not taken into account in the calculations of Oliveira-Pinto et al. (2019).*

4.3 Value Adjusted Levelized Cost of Electricity

This section presents the results of both VALCOE-calculations done in this research: the Value Adjustment and the Capacity Adjustment.

4.3.1 Value Adjustment

The value adjustments of both locations is presented in Figure 4.5. As can be seen, for both locations and all devices, the Value Adjustment is positive, meaning that the devices operate more during peak hours when the Day-Ahead Price is higher compared to the system average. For Lysekil, a carbon tax and certificate trading system is in place, that for 12.7 dollar/MWh is responsible for the Value Adjustment. Removing that will significantly lower the Value Adjustment for Lysekil, but it will still remain positive. This is likely due to the calmer wave climate at Lysekil: a less energetic wave climate will, also during peak hours, cause less revenue. The UK has no support schemes into place, so the Value Adjustment shown is purely the effect of WECs operating during peak hours.

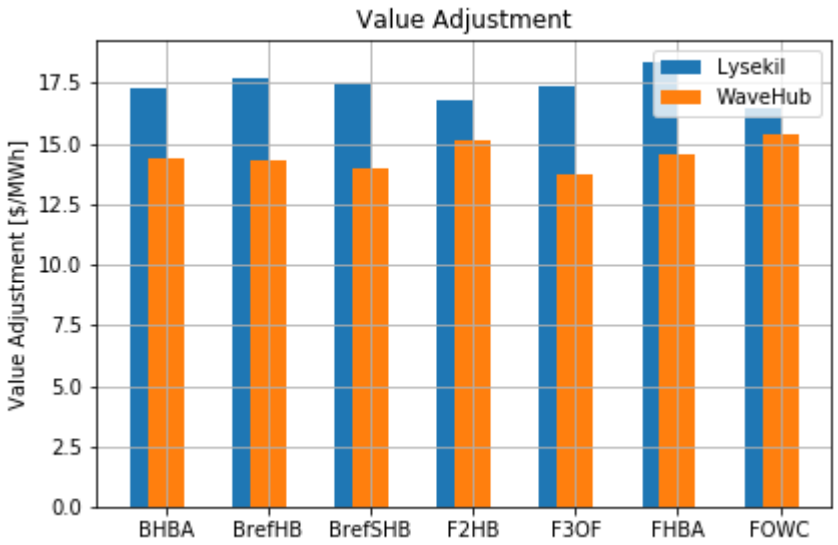

Figure 4.5: *Value Adjustment values for both locations. Note that the VA on Lysekil includes the carbon tax and FIT present in Sweden. Removing those would still let the VA of Lysekil be positive, but much closer to zero.*

4.3.2 Capacity Adjustment

The resulting surplus probability density functions for Sweden and the UK are presented in respectively Figures 4.6 and 4.7. The resulting Z-method statistics are summarized in Table 4.6.

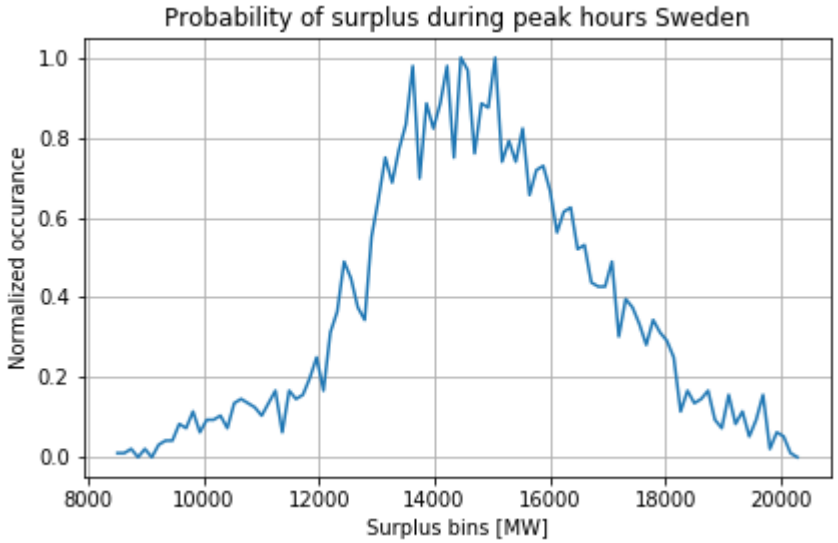

Figure 4.6: *Probability Density Function constructed for the Z-method of Sweden.*

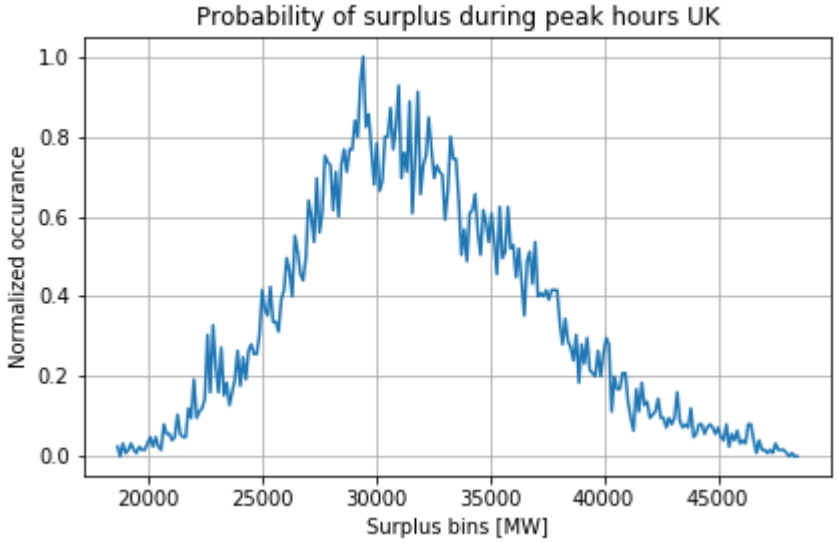

Figure 4.7: *Probability Density Function constructed for the Z-method of the UK.*

As can be seen from Figures 4.6 and 4.7 and Table 4.6, both countries have a power system in place in which a lot of surplus is present, even using a conservative calculation with subtracting imports and the Largest Infeed Loss (LIF), defined as the largest power plant present in the countries electricity system. This is reflected by the high Z-fraction listed in Table 4.6. In Dragoon and Dvortsov (2006), Z-values of around 1-2 are used as examples, meaning that the

Table 4.6: *Z-method coefficients.*

	Sweden	*UK*
Expected Surplus (mean) [MW]	14456	29450
Standard Deviation [MW]	2027	5132
Z method adequacy 'Z' [-]	7.13	5.74

expected surplus is only one or two standard deviations away from zero.

The resulting capacity credit, in MW per MW installed, and the capacity adjustment values, are presented in Figures 4.8 and 4.9.

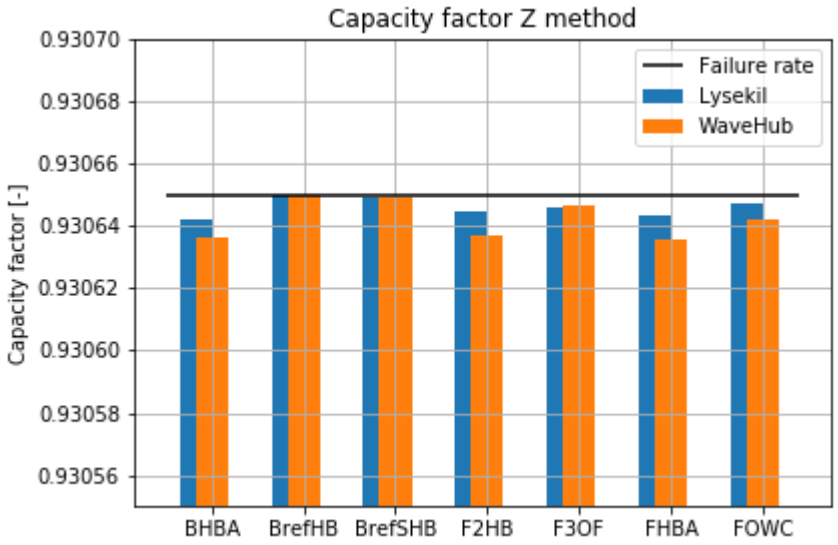

Figure 4.8: *Calculated Z-fraction using equation 2.12. The horizontal line shows, the known availability, computed as 1 - unavailability rate.*

As expected from the results from the Z-method presented in Table 4.6, the main part determining the capacity factor shown in Figure 4.8, is the failure rate. The other contribution, coming from the added variability to the system by implementing the WECs, is very small. This has two causes: 1) the electricity systems in both countries have an enormous surplus in the order of 10 GW, while the largest WEC to be analyzed in this research has a rated output of 2.7 MW and 2) the variability of WECs is relatively low compared to that of for example offshore wind and solar PV. This will be further elaborated on the next section.

The previous analysis considered one device of every kind installed at both locations. The WEC with the largest rated power is the BHBA, at 2.7 MW. This does not come close to the surplus of 10-30 GW and installed capacity of 70-100 GW in both countries. The analysis is repeated for the integration of 5 MW and 5 GW of wave power into both countries system. The resulting Z-fractions are presented in Figure 4.10 and 4.11.
The results in Figures 4.10 and 4.11 show that for increased integration of WECs into both energy systems, the fraction with which the load can be increased decreases. This can also be deducted from Eq 2.12. I_c is in the denominator, while σ_R^2 is in the numerator. Increasing the number of WECs installed in this research is done by multiplying the power output by the

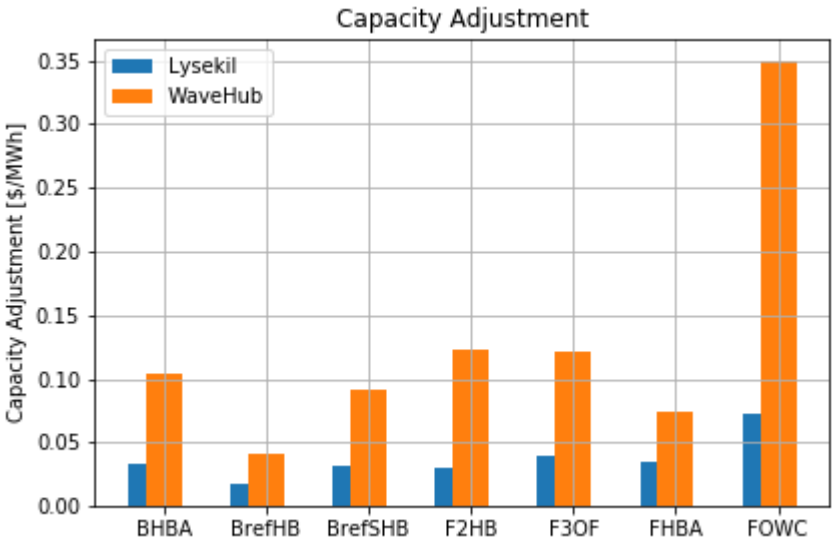

Figure 4.9: *Capacity adjustment calculated using the results from the Z-method shown in Figure 4.8 and based on equation 2.6.*

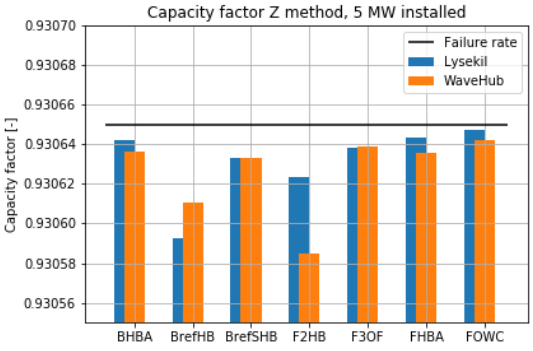

Figure 4.10: *Z-fraction for integrating 5 MW of wave power into both energy systems.*

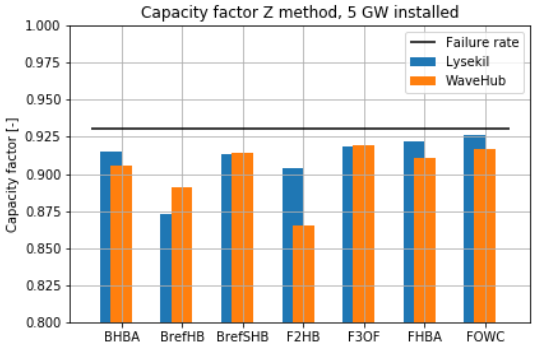

Figure 4.11: *Z-fraction for integrating 5 GW of wave power into both energy systems.*

desired number of WECs installed. Since no hydrodynamic effects of multiple WECs are taken into account at this point, I_c and σ_R are linearly scaled with the amount of WECs installed. Since σ_R in the numerator is squared, the total Z-fraction is linearly dependent on the amount of WECs installed.

It has to be noted that the Z-method is not developed for modelling large scale integration of variable techniques: for larger integration the Z-method solution starts to deviate from the results obtained by energy system model calculations. Keane et al. (2010) tested this for large scale wind generation integration in the UK and found that the Z-method starts to deviate from the preferred iterative COPT (Capacity outage probability table) method after a few GW installed capacity, so the calculations with 5 GW added WEC capacity are less trustworthy than the calculations done with 5 MW and for single device integration. They should be interpreted as indications.

4.4 Variability

There are several studies suggesting that wave energy is less variable compared to offshore wind, onshore wind and solar PV (see for example Astariz and Iglesias (2016b) or Fig 2. in Widén et al. (2015)). Using the power matrices and sea state time series, power production time series were created for this research, which can be used to compute the variability. Furthermore, the Open Power System Database (OPSD, 2020) used contains timeseries on the total wind power and solar PV generation for both countries.

Having multiple WECs installed at the same spot will lower the variability of the power output, because of the different machines catching waves at different times, but due to hydrodynamic interactions also the total power output will be lower (Göteman et al., 2015). Göteman et al. (2015) modelled this for 1 and 100 Bref-HB devices deployed at the same test site at Lysekil as used in this research. The ratio in variability between 1 and 100 devices from Göteman et al. (2015) is used to get ballpark values of the variability decrease caused by upscaling.

The resulting variability of wind power and solar PV generation from the OPSD (2020) dataset, the variability of the devices in this research and the correction for 100 devices using the results of Göteman et al. (2015), are summarized in Tables 4.7 and 4.8. The variability values are calculated by dividing the standard deviations by the mean to make comparison possible.

Table 4.7: *Variability of wind power and solar PV generation, originating from data from OPSD (2020) and wave power, calculated from the timeseries in this research. For Solar PV, only the daytime hours are taken into account.*

	SOLAR		**WIND**					**WAVE**	
	UK	*SE*	*UK (Total)*	*UK(Offshore)*	*UK(Onshore)*	*SE(Total)*	*SE(Onshore)*	*UK*	*SE*
SIGMA/MEAN	1,02	2,8	0,86	0,35	0,54	1,12	0,60	0,84	1,43

According to the results presented in Table 4.7 the variability of wave power is lower than the variability of solar PV in Sweden, but more variable compared to wind power generation and solar PV generation in the UK. However, the results for wind and solar PV are based on production timeseries of all wind and solar PV installed in both countries, while the variability of wave power generation is based on the deployment of a single device in a single location.

Table 4.8: *Variability of one BrefHB machine from data published by Göteman et al. (2015), calculated by using a power matrix (PM), for 100 devices installed at Lysekil, computed by Göteman et al. (2015) and the ratio of 1/100 devices applied to the average variability of wave power output calculated in this research in both countries.*

Bref-HB	1 device (Göteman et al., 2015)	1 device (using a PM)	100 devices (Göteman et al., 2015)	Ratio	Sweden, with ratio	UK, with ratio
SIGMA/MEAN	1,37	1,10	0,46	0,34	0,48	0,28

Based on Table 4.7 it can thus be stated that a single WEC deployed on either location already has a lower variability compared to all solar PV systems installed in the respective countries.

The first thing to notice on Table 4.8 is that the variability of one Bref-HB device calculated by Göteman et al. (2015) is slightly higher than the one calculated in this research by using power matrices. A power matrix is in a sense a summary of the power production specifications of a WEC system, and by summarizing the power production properties into such a matrix, some of the variability is lost. Göteman et al. (2015) did not use power matrices but relied on direct hydrodynamic modelling. Secondly, the variability of the power production of 100 Bref-HB devices is rouhgly 3 times as low as the variability of 1 Bref-HB devices. Using this ratio on the values for 'Wave' from Table 4.7 gives an indication what the variability looks like when multiple WECs are installed in both countries. According to this calculation, the variability of deploying 100 WECs is lower than the total wind power and solar PV production in both countries.

5 Results: Case studies

Two case studies are considered in this research. The first case study consists of a wave park of 100 Bref-HB machines deployed at Lysekil, using scale factors to decrease the values for the CAPEX and OPEX and interference to decrease the power output based on the work of Göteman et al. (2015). The second case study is the integration of all seven devices in the smaller energy system of Malta, an island in the Mediterranean sea.

5.1 Wave park Lysekil

Göteman et al. (2015) found, in a model study with the wave climate of Lysekil, that increasing the number of WEC devices from 1 to 100 Bref-HB systems increased the power output from 12 kW to 947 kW, which is 79 % of the output one would expect if the devices would not interact. Also, Göteman et al. (2015) modelled the variability of 1 and 100 devices, and from the time series of the power output could be computed that, when using 100 Bref-HB devices, the variability in power output decreased to 33 % of its original value, see Table 4.8.

There are multiple studies done on the effects of interacting WECs in a park, both numerical (for example by Borgarino et al. (2012), Giassi and Göteman (2018) and Ruiz et al. (2017)) and experimental (for example by Giassi et al. (2020b) and Fonseca et al. (2016)). The value used in this research to decrease the energy output of several WECs is the lowest one found in the literature. A value closer to 1 is more common, and even a value larger than 1 because of positive interference is possible when several WECs are placed in a park, for example shown by the model study of Wu et al. (2016). This is not part of the calculations in the previous sections: no interference was previously assumed.

It can be reasonably expected that the CAPEX per kW installed will go down because of scaling effects, or the possibility to combine cables and substations for several devices. Also, increasing the number of WECs could decrease the OPEX, because operational activities like repairs can be done for multiple devices at the same time. Giassi et al. (2019), who based their CAPEX assessment on the work of Ericsson and Gregorson (2018), is used here to determine the decrease in CAPEX and OPEX. No exact numerical values were available, so the decrease in CAPEX and OPEX is assessed from the Figures in Giassi et al. (2019) to be between 25 % and 50 %. In this study, 40 % is chosen as CAPEX and OPEX decrease factor, assuming that they both decrease with the same factor.
The resulting change in metric values is presented in Table 5.1.

Table 5.1: *Calculated metrics for 1 and 100 devices deployed at Lysekil, showing the trade off between lower CAPEX and OPEX and power production.*

Variable name		1 device	100 devices	Difference
LCOE	*$/MWh*	711.67	360.34	-49.4 %
PBP	*years*	128.2	95.7	-25.4 %
Value Adjustment	*$/MWh*	17.51	17.51	0
Capacity Adjustment	*$/MWh*	0.052	0.066	26.6%

As can be concluded from Table 5.1, the effect of the decreased CAPEX and OPEX is stronger than the effect of the decreased power output of the Bref-HB, reflected by the lower LCOE and PBP for 100 devices. The value adjustment does not change, since it is only dependent on the moment of power generation, which is determined by the wave climate time series and does not change. The Capacity Adjustment increases with 26%. As can be seen in Equation 2.6, the capacity adjustment is linearly dependent on the fraction capacity credit over capacity factor. The capacity credit, calculated by the Z-factor, increases because of the lower variability in the wave park compared to a single device. The capacity factor decreases because the power output per device decreases in this case study. This combined effect makes the capacity adjustment increase for a wave park compared to a single device.

5.2 Malta

Malta is an island and micro-state in the southern part of the Mediterranean sea, between Sicily and the African coast (see Figure 5.1). The direct access to the sea and the small power system present on Malta would intuitively make wave power attractive to integrate, but the effect the integration of the variable renewable energy source has on the Maltese power system might be larger than the effect on larger power systems like the ones present in Sweden and the UK, because of the likely smaller surplus. No Day-Ahead price, FIT or base capacity value could be found for Malta, so a direct comparison of Malta with the UK and Sweden in terms of the PBP, value adjustment and capacity adjustment is not possible.

Figure 5.1: *Malta and its location in Europe, adapted from Bugeja (2020).*

In 2019, the total installed capacity at Malta was 689 MW, of which 200 MW is the interconnecting cable to Sicily (Bugeja, 2020). This cable is almost solely used for importing electricity from the Italian power system to Malta, export almost never happens (Bugeja, 2020). The cable is of vital importance for the Maltese power system: as the result of a dropped anchor the cable was out of operation at the end of the summer in 2019, which caused power outages for weeks (Nexans, 2020).

From private communication with Bugeja (2020), based on the information of the Maltese TSO, a daily average load profile in MW per hour and the monthly load in MWh could be obtained. Data with a higher resolution was not available because of confidentiality restrictions by the TSO. By using fraction X of monthly load and average monthly load, a factor per month could be obtained. For example, let the annual average monthly load be 100 MWh, and the monthly load for July and August be 110 and 90 MWh respectively. July then gets a fraction X of 1.1, August a fraction X of 0.9. It can then be assumed that, by multiplying the daily average load profile with this fraction, the average daily load profile per month could be approached. Furthermore, if it is assumed that this fraction happens at the middle of every month, and that the fraction increases or decreases linearly per month, the daily average load profile could be interpolated. This results in 365 different 24 hours daily load profiles, corrected for the total monthly consumption. Note that the shape of the daily load profile remained roughly equal.

The largest power plant currently operative on Malta is a Combined Cycle Gas Turbine (CCGT) of 180 MW (Bugeja, 2020), and is used in this research as the Largest Infeed Loss (LIF) of Malta. Furthermore, the daily import profile was not available, but Bugeja (2020) mentions three practical import levels as percentage of the daily load: 20 %, 37 % and 60 %. These levels are used in this research as import rates as well.

Combining the daily load profile, the LIF and the three import scenarios with the definition of the peak hours (between 8:00 - 14:00 and 16:00 - 22:00, see Fig 18 in Bugeja (2020)) and the peak months (January, July, August and September, see Fig 17 in Bugeja (2020)), gives for the three import scenarios the surplus. The surpluses are shown in Figure 5.2.

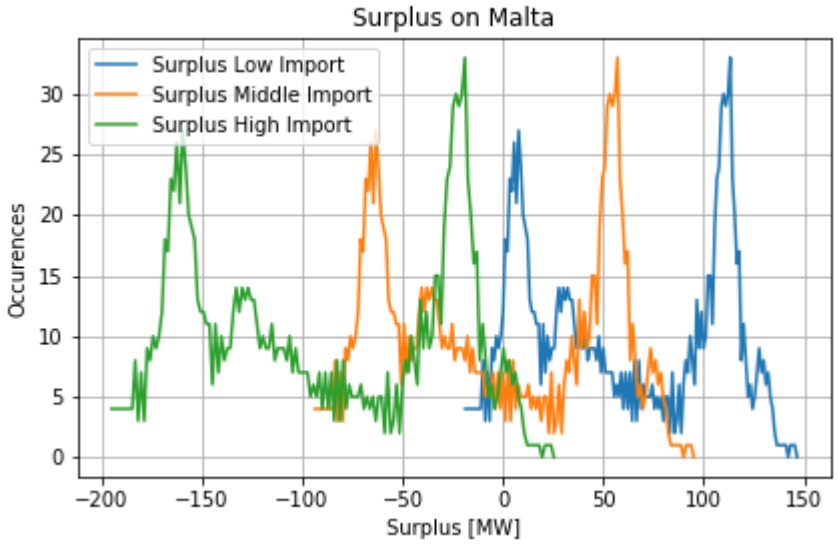

Figure 5.2: *Surplus on Malta for the three import scenarios of 20%, 37% and 60% for respectively the Low Import, Middle Import and High Import scenario.*

The High import scenario has an expected surplus S_0 below zero. The Z-method from Dragoon and Dvortsov (2006) cannot deal with expected surpluses below zero, as the fraction to be subtracted from one is then negative, making it possible to increase the load of the system by more than the maximum installed capacity. Therefore, in this research, the High Import scenario is discarded.

Wave data for Malta could be retrieved from the MEDSEA Hindcast model from 2012-2019 (Korres et al., 2019), in the form of hourly time series of H_s and T_p. A few grid points were tested, and a grid point from the MEDSEA Hindcast model 15 km south of the South-eastern point of Malta is chosen, because of the most energetic sea compared to other points around Malta. The sea state probability matrix is presented in Figure 5.3. The difference in LCOE between Malta and Lysekil and Malta and WaveHub is presented in Figure 5.4.

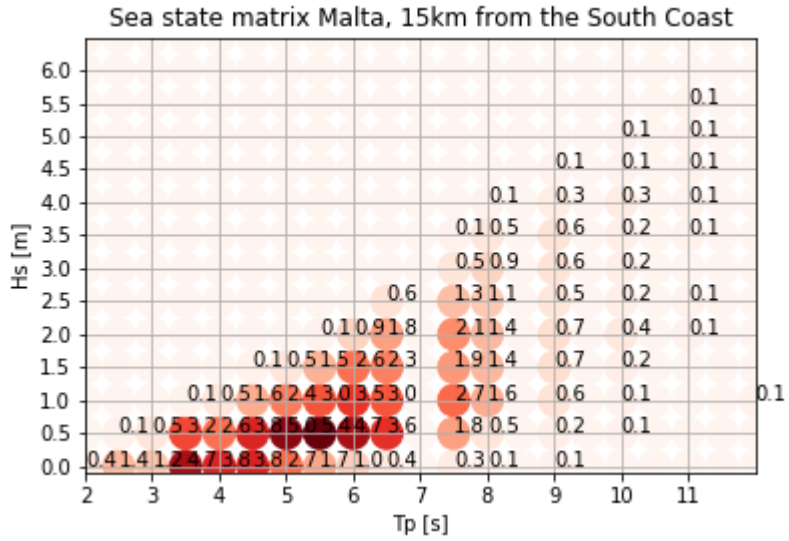

Figure 5.3: *Sea state Matrix for a gridpoint of the MEDSEA Hindcast model (Korres et al., 2019) 15 km south of the most south eastern tip of Malta.*

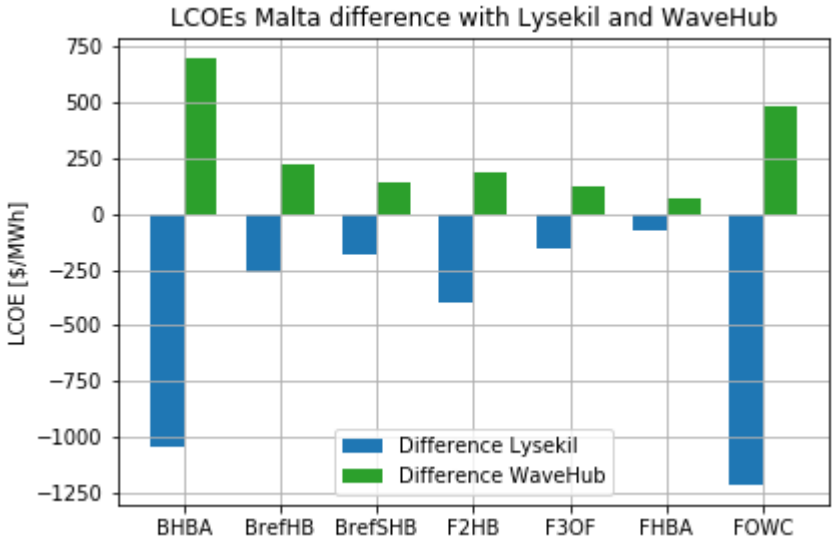

Figure 5.4: *LCOE of Malta compared to the ones computed for Lysekil and WaveHub (LCOE Malta - LCOE location).*

The sea state at Malta presented in Figure 5.3 shows that wave climate is more energetic (more likely to find combination of high H_s and T_p) than the wave climate of Lysekil (see Figure 3.6) but less energetic (less likely to find combination of high H_s and T_p) compared to the wave climate of WaveHub (3.3). This is reflected in the results of the LCOE comparison, presented in Figure 5.4, for all devices the LCOE computed with the wave climate of Malta is in between the LCOEs computed using the wave climate from Lysekil and WaveHub.

The calculated Z-fractions per device for both the middle and low import scenarios are presented in Figures 5.5 and 5.6. As expected, because Malta has a smaller power system and a lower surplus, the Z-fraction is smaller and less power per WEC can be used to increase the load compared to integration in Sweden and the UK. However, for both 1 device and 50 MW integration, the middle import scenario has a larger Z-fraction. This is caused by both a lower expected surplus $S0$ and slightly higher standard deviation of surplus σ_s, both making the contribution of the second term on the RHS in equation 2.12 smaller, and therefore the final fraction to be used, without decreasing the reliability of the system, larger.

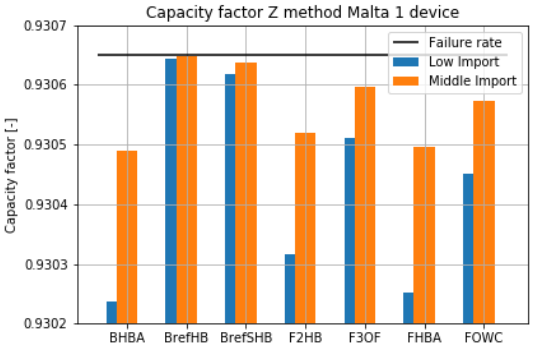

Figure 5.5: *Z-fraction for integrating 1 device of every WEC into the Maltese power system, for the low and middle import scenarios.*

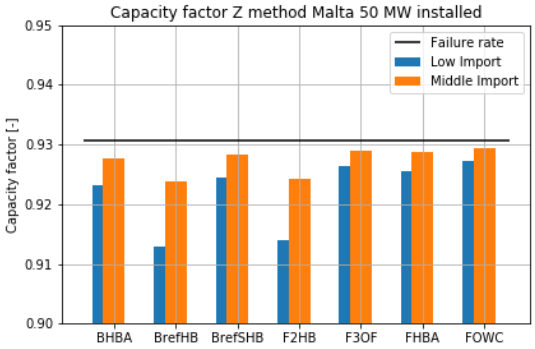

Figure 5.6: *Z-fraction for integrating 50 MW of wave power into the Maltese power system, for both import scenarios.*

Again, the same side note has to be made as for the 5 GW integration in the Swedish and British electricity system: the Z-method is proven to work for small integration of a variable renewable energy source, for larger integration the solution starts to deviate from the energy system models. 50 MW is in the Maltese power system already a significant part of the surplus, so these results are less reliable.

6 Results: Monte Carlo analysis

For the Monte Carlo analysis, three input variables are varied: the CAPEX, the OPEX and the power matrices. The CAPEX and OPEX are multiplied with a factor between 1 and 6, because a sixfold of the CAPEX and OPEX used in this research has been found in the literature. The probability density functions used to pick the multipliers for the CAPEX and OPEX are chosen to be right tailed. This is done because more literature could be found with values close to the ones used in this research than to the sixfold. The probability density functions of both multipliers are presented in Figures 6.1 and 6.2.

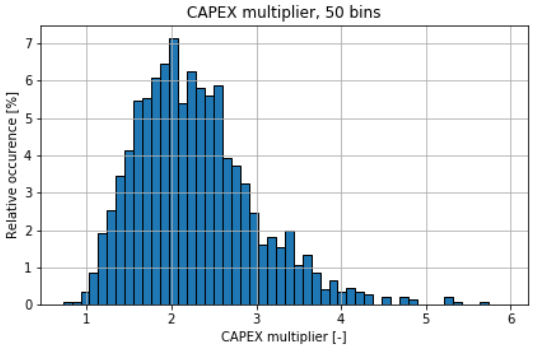

Figure 6.1: *Probability function of the CAPEX multiplier as input for the Monte-Carlo analysis.*

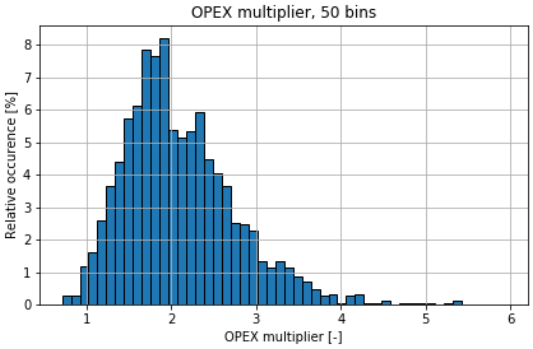

Figure 6.2: *Probability function of the OPEX multiplier as input for the Monte-Carlo analysis.*

The power matrices are varied using the same way as for the CAPEX and OPEX: the used probability function is presented in Figure 6.3. The PDF in Figure 6.3 is left tailed, because all power matrices found in the literature had higher power outputs compared to the ones used in this research. The value is then used as in Equation 6.1, in which $PM*$ is the new power matrix, PM the old one, f the factor from the PDF and IC the installed capacity, so that the value on every grid point of the power matrix can never exceed the rated capacity of the device.

$$PM* = min(PM*(1+\frac{f}{100}), IC) \tag{6.1}$$

Then, using the PDF's from Figures 6.1, 6.2 and 6.3, the model was run 1800 times. The output of the Monte Carlo analysis consists of a matrix with dimensions 1800 (amount of runs) x 10 (metrics) x 7 (WECs). The results are then summarized by first converting the output in numerical values to a percentage change with respect to the values originally calculated and presented in the previous chapter. Then, the mean and standard deviation per WEC per metric is computed. Then, the mean percentual change and standard deviations of all seven devices are averaged and used to compute per metric one 95 % confidence interval (using for the boundaries $CI = X_{mean} \pm Z\frac{s}{\sqrt{n}}$, in which X_{mean} is the mean of the variable to be considered, Z the statistical multiplier, being 1.96 for 95 % CI intervals, s the standard deviation and n the number of samples).

This way of presenting the output is mainly chosen to decrease the amount of datapoints to be shown, but by doing so, one loses the specific effects of different WECs and corresponding power matrix. To counteract this, two WECs with largely different power matrices are highlighted using the same approach. The highlighted WECs' power matrices, the narrow-peaked BrefHB power matrix and the broad-peaked FOWC power matrix, are presented in Figures 6.4 and 6.5.

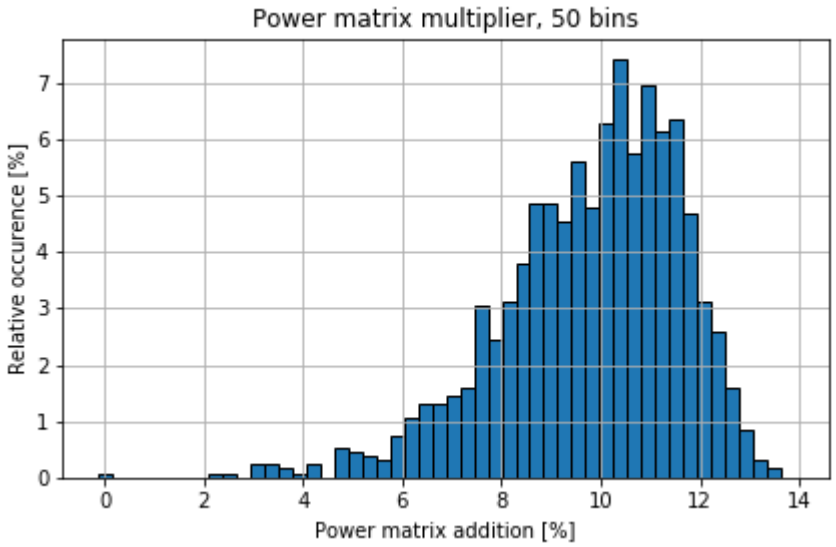

Figure 6.3: *Probability density function used to determine the multiplier for the power matrices.*

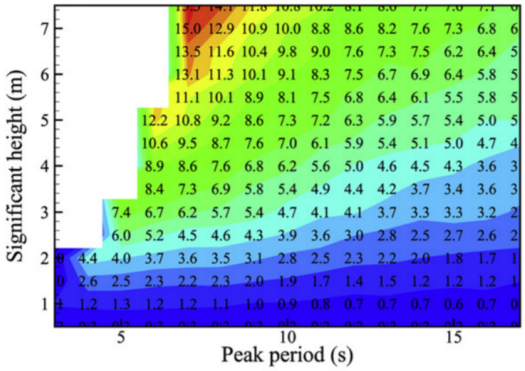

Figure 6.4: *Power matrix of the Bref-HB device, adapted from Babarit et al. (2012).*

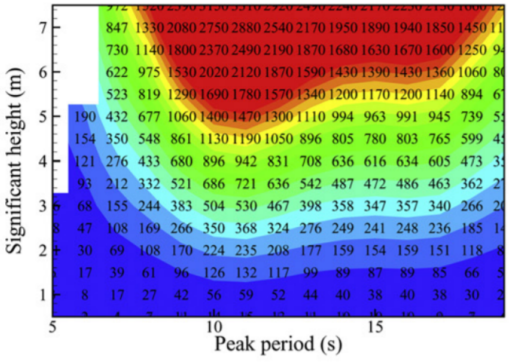

Figure 6.5: *Power matrix of the FOWC device, adapted from Babarit et al. (2012).*

The general averaged output, expressed in percentage changed from the original values, is presented in Figure 6.6. The values for the Bref-HB and FOWC are presented in Figures 6.7 and 6.8. The numerical values displayed in these figures are presented in Table 6.1.

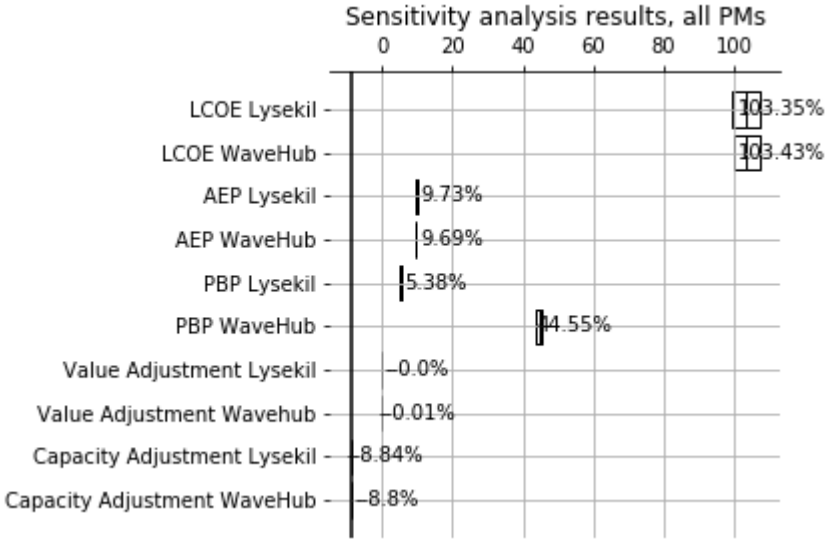

Figure 6.6: *Percentage changes on average from the Monte Carlo analysis, including (very narrow) confidence intervals.*

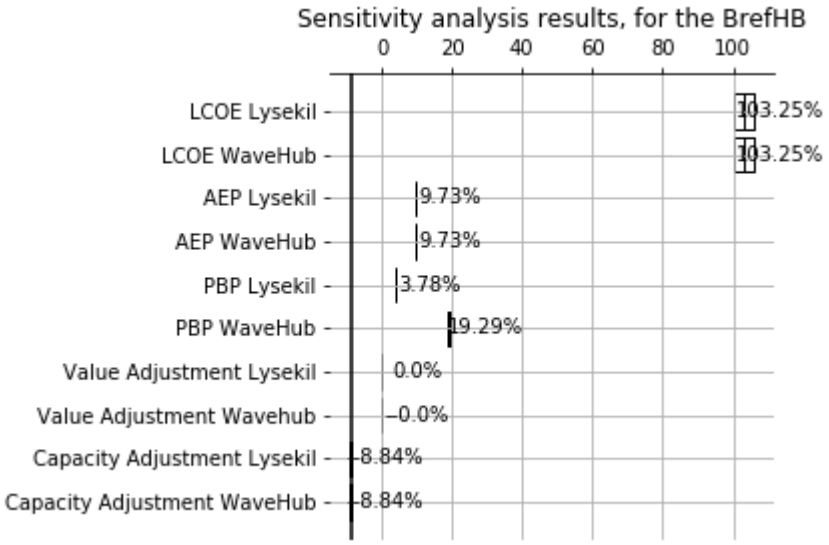

Figure 6.7: *The Monte Carlo analysis output of the Bref-HB device.*

The confidence intervals of almost all metrics are very narrow. This is likely because a higher power output of the WECs, simulated in the Monte Carlo analysis by multiplying the power matrices with a factor, has the opposite effect as increasing the CAPEX and OPEX. Also, the power output on average increases by 10 % in this Monte Carlo analysis, the CAPEX and OPEX

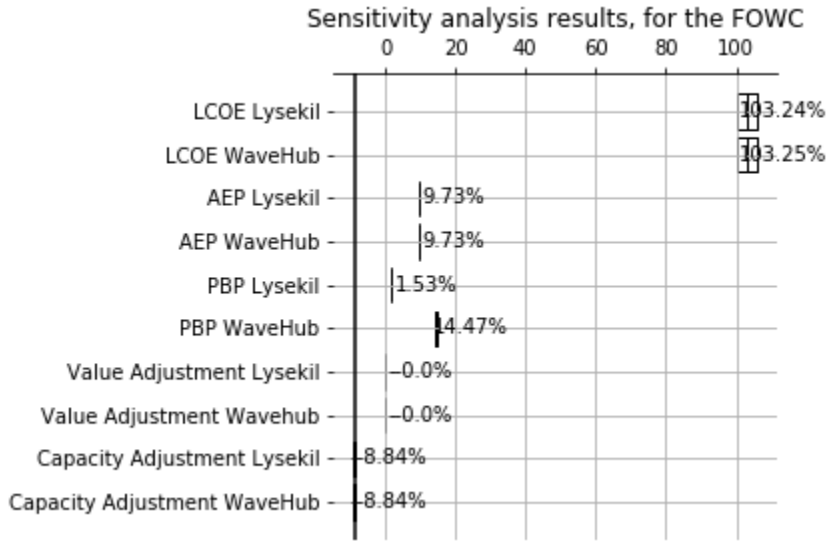

Figure 6.8: *Monte Carlo analysis output of the FOWC device.*

Table 6.1: *All numerical values of the 95% confidence intervals in percentage, from Figures 6.6, 6.7 and 6.8.*

Metric	General (fig. 6.6)		Bref-HB (6.7)		FOWC (fig. 6.8)	
-	*lower*	*upper*	*lower*	*upper*	*lower*	*upper*
LCOE Lysekil	99.6	107.1	104.3	106.1	100.4	106.1
LCOE WaveHub	99.7	107.2	104.3	106.1	101.0	106.1
AEP Lysekil	9.61	9.85	9.64	9.82	9.64	9.82
AEP WaveHub	9.57	9.80	9.64	9.82	9.63	9.82
PBP Lysekil	5.26	5.29	3.70	3.86	1.44	1.62
PBP WaveHub	43.7	45.4	19.0	19.5	14.3	14.6
Value Adjustment Lysekil	0	0	0	0	0	0
Value Adjustment WaveHub	-0.01	-0.009	0	0	0	0
Capacity Adjustment Lysekil	-8.93	-8.74	-8.91	-8.76	-8.91	-8.76
Capacity Adjustment WaveHub	-8.90	-8.70	-8.91	-8.76	-8.91	-8.76

are on average multiplied by 2 (100 % increase), so the increase in power output is easily offset by the increase in costs.

The LCOE is expected to increase for all devices and both locations with over 70 %. This means that, according to Figure 4.4, the values of the LCOE for WaveHub are expected to be closer to the ones computed by Oliveira-Pinto et al. (2019).

The pay back period seems to be the only metric that has different values per device and per location. The effect is stronger on the WaveHub site compared to Lysekil. This is likely because the wave climate at Lysekil already caused the PBPs to be low, likely because of sea states outside of the power matrices (e.g. too low to be picked up by the WECs). A change in power matrix or costs will then do less to the calculated PBP.

In the overall results from the Monte Carlo analysis, there are small differences between the two locations in the mean and range of the confidence interval. For the Bref-HB, they are per location exactly the same, but for the FOWC they deviate a little. This is likely caused by the small shape change of the power matrix as a result of the multiplication factor. If the values in the original matrix are close to the total installed capacity, often in the 'red' area in the power matrix, they might be capped off by the installed capacity instead of being raised with the factor from the PDF. This causes values in the 'red' area of the power matrix to change less than the values in other spots, thereby altering the shape of the power matrix. If the 'red' area is larger and/or close to combinations of H_s and T_p that are likely to happen, one would expect a difference in the reaction to different sea states. The FOWC has a larger 'red' area compared to the Bref-HB, so it is expected that the power matrix shape changes more, and therefore the confidence interval per location starts to deviate.

The change in Value Adjustment is zero, although the power matrix functions as an input for this calculation. This is because the Value Adjustment is an average based on the times of production. More production means more power output, and also a higher revenue, leading to no change in the MWh/$ ratio. The Value Adjustment is therefore only dependent on when the devices operate, which is determined by the sea states and the shape of the power matrix. The shape of the power matrix can theoretically change a little bit in this Monte Carlo analysis, because Equation 6.1 dictates that the maximum value can never exceed the rated power of a device. However, this will only happen for combinations of large H_s and long T_p, an area in the power matrix almost never reached for both locations. This likely causes the very small and narrow confidence interval in WaveHub, as in that spot those wave conditions can happen.

The capacity adjustment decreases in this Monte Carlo analysis. According to Equation 2.6, it is dependent on three variables: the capacity credit (the Z-value in this research), the base capacity value and the capacity factor. The base capacity value is not changed in this Monte Carlo analysis, the capacity factor increases because the power matrices are being upscaled, and the Z-fraction might change due to a changing power matrix. Since for all cases the percentual change is negative, it can be concluded that the increase in capacity factor in the denominator has a stronger effect than the change in the Z-factor in the numerator. However, if there would only be an effect of the capacity factor, one would expect that the decrease in capacity value would equal the increase in the average energy production, since the capacity factor is directly calculated from the AEP. This is not the case: there is roughly a 1% in the absolute value of the confidence intervals of the AEP and the capacity adjustments, meaning that this 1% decrease can be attributed to the decrease in variability, which is likely caused by a slight change in the shape of the power matrices.

7 Discussion

The power matrices used in this research originate from a publication in 2012. The market for and the development of WECs is rapidly changing so these power matrices are likely not fully representative of for WECs developed today. WECs that are developed more recently would likely have on average a higher power output. This would explain the average negative bias the power matrices have compared to matrices in other, more recently published articles.

Mérigaud and Ringwood (2018) argue that the use of power matrices is an oversimplification of the power production of WECs, leading to errors. It was outside the scope of this research to simulate the power production of the WECs from scratch, but doing so would likely increase the reliability of the calculated metrics. In particular, including state-of-the-art control methods designed to enhance the energy absorption (see for example Wang et al. (2015)), and therefore approach reality better, would dramatically increase the power absorption and thereby reduce the LCOE.

The calculated LCOE is in line with the ones published by Oliveira-Pinto et al. (2019), who use the same CAPEX and OPEX, and the same power matrices. This confirms the calculations done in this research, but the assumption that the CAPEX and OPEX are the same for both sites remains. As mentioned in section 4, one could expect both higher CAPEX and OPEX at sites with more energetic wave climates. It is beyond the scope of the current work to consider this, but the assumption might lead to biased conclusions in favor for WaveHub, as only the positive aspects of an energetic wave climate are taken into account.

There is a large difference between the LCOE of the devices, likely due to the differently shaped power matrices that favour different wave climates. For WaveHub, the LCOE is in the range 100-1000 $ per MWh for a single WEC. According to the latest world energy model (IEA (2020a)), the LCOE of various energy sources is between 10 - 200 $ MWh, with the lowest LCOEs in Europe being 65 $ per MWh for Gas CCGT and the highest LCOE for Nuclear at 155 $ per MWh. In this study, wave energy has an higher LCOE compared to existing energy sources. This research takes a single device of every kind into account, installing a full park of several devices will lower the CAPEX and OPEX, while also lowering the power production per device a little (see for example Göteman et al. (2015)), but in general the LCOE is believed to go down when scaling up the number of WECs. This is tested for 100 Bref-HB devices at Lysekil, see chapter 5, and the same trend is expected for all other devices.

The capacity factors are low compared to other renewable energy sources, ballpark values for offshore wind are for example 0.25 - 0.5 and 0.3 for solar PV. To test if the low capacity factors of wave energy are the result of general low power production or the result of a lot of occurrences of unsuitable sea states with no power production, all timesteps in the PBP calculation where the power production of the WECs is nonzero are counted and divided by the total amount of timesteps to obtain a 'power production temporal percentage'.

There are two occasions when the power output of a WEC is zero: 1) when the combination of H_s and T_p in the power matrix has zero kW as output and 2) when the combination of H_s and T_p falls outside of the power matrix. By only taking into account 1) all devices except the FHBA had a power production temporal percentage of 1, meaning that every timestep that the sea state was withing the boundaries of the power matrix, the WECs were able to produce power. The FHBA's power production temporal percentage is 98 % and 99 % for respecitvely Lysekil and WaveHub. Taking 2) into account as well, the values of all devices became 93% and 99% for respectively Lysekil and WaveHub. This leads to the conclusion that for the vast majority

of the sea states used in this research, the WEC devices were able to produce power and the low capacity factor is purely the result of low power production, but nonzero power production, during most of the timesteps.

The PBP of all devices seems to not be reached during the lifetime of the WECs at Lysekil. This is due to the low energy output. This was expected: the wave climate is not extremely energetic at Lysekil, compared to WaveHub, so revenues will be low. Larger energy absorption (e.g. due to control methods) and/or lower costs (e.g. due to shared infrastructure in parks) would obviously increase the revenue.

The Value Adjustment, being clearly defined by the IEA as the difference between revenue of a generator and the revenue of the system, is positive for all WECs on all locations. For Lysekil, this is heavily influenced by the certificate system and the carbon tax, which give it an advantage over other conventional generators in the system that rely solely on the Day-Ahead price for revenue. For WaveHub, no such schemes are in place however the value adjustment is still positive. This highlights that wave power is mainly generated during peak hours when the day-ahead price is high. Further research could be on the correlation between the Day-Ahead price and energetic sea states. It is expected that at locations where this correlation is high, the profitability of WECs will also be high.

The surpluses in electricity supply in both countries are determined in a conservative way, by assuming a largest in-feed loss and by excluding import from the calculation. Still, the surpluses are considerable, being in the order of 10-100 GW, with no expected loss of load in both countries.

In the calculation of the surpluses, there is no distinction made between renewable and fossil based installed capacity: 1 MW of installed offshore wind generation is counted the same as 1 MW of installed CCGT. In reality, the CCGT power plant can be turned on or off, thereby almost immediately responding to changes in the load pattern. An offshore wind turbine can obviously not do that. Therefore, when computing surpluses in the electricity system to use as input for adequacy calculations, some method has to be used to correct the installed capacity for variable energy sources. This can either be done by considering the average capacity factor of the renewable sources installed, or by considering the variable renewable generation as time series like the electricity import rather than it being treated as fixed installed capacity.

There are multiple definitions used as 'peak hours' in the literature, differing per country. Using different definitions of peak hours did change the resulting surpluses significantly. Different peak hour definitions makes it hard to compare results with other studies. It would be convenient if there was a common method of defining the peak hours, for example endorsed by the IEA. This definition can then rely on statistics of the daily load profiles and outside temperatures during weekdays in combination with the gas consumption to rule out gas-fired heating systems.

The Z-method power production fraction is to a very large extent determined by the unavailability rate, and only for a very small portion by the added variability to the energy systems. This is due to the enormous surplus (10-100 GW) and the integration of at max 2.7 MW for the device with the highest rated power (BHBA). The surplus is therefore at least thousandfold the added capacity, adding this capacity will almost do nothing to the system's adequacy. Dragoon and Dvortsov (2006) stress in their study that for low integration of a technology into the energy system the Z method gives results close to the computational expensive energy systems models calculations, it starts deviate from the model results when more integration is considered. Therefore, the tests with larger integration in this study should be interpreted as indications.

The deviation from complex model solutions is mainly because the key assumption of the Z-method is that the characteristics of the energy system, summarized in the mean and standard deviation of the surplus, do not change because of the integration of a new generation source. For large amounts of variable energy generation, one could reasonably expect that the surplus will change significantly. A possible way to tackle this, is to compute the Z-method in steps. Take for example the integration of 1 GW of rated WEC power into the system, with corresponding standard deviation. 1 extra GW of WEC power will likely alter the surplus significantly: both its mean and standard deviation will likely change. One could divide the integration of 1 GW into steps of 10 MW and a corresponding percentage of the standard deviation, and after each step recalculate the new surplus of the system, taking into account the Z-fraction of the added 10 MW. This process is schematically shown in Figure 7.1. Further research could test the iterative solution presented in Figure 7.1 on the difference with one step, the effect of different step sizes, and the computational expense. The latter is expected to increase significantly, as for every iterative step, the surplus has to be recalculated.

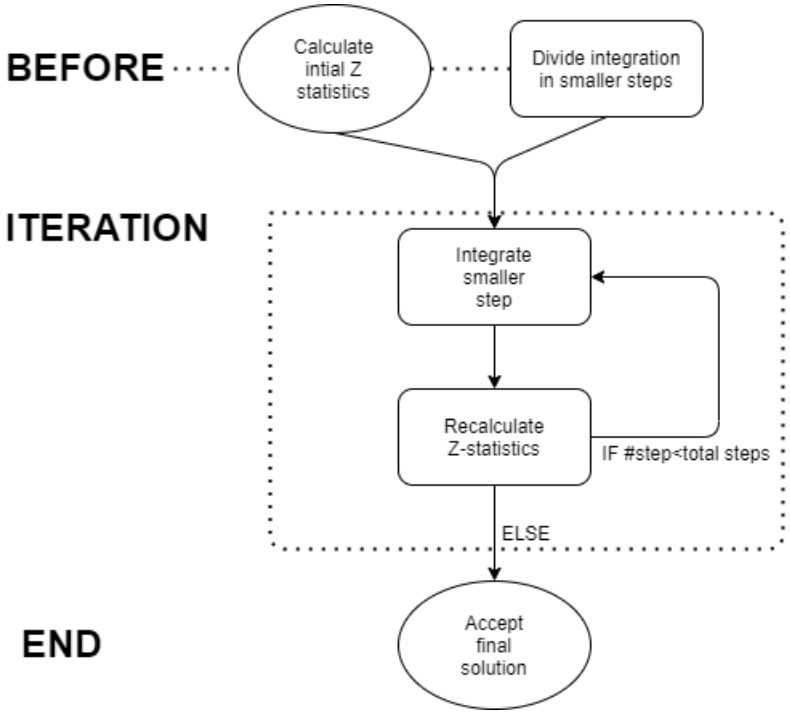

Figure 7.1: *Iterative solution scheme of integrating a larger amount of variable power generation in steps, while allowing the surplus and therefore the Z-statistics to change in between steps.*

The variability calculations were done using the results from a study on a single device deployed at a single location, and projected on 100 devices of the same kind. Furthermore, the results from the study of Göteman et al. (2015) are based on hydrodynamic calculations, and then projected on calculations made by using power matrices in this study. The trustworthiness of the exact numbers is therefore expected to be low, but the general trend of a lower variability of WECs compared to offshore wind and solar PV is in line with earlier studies, and is judged to be credible.

The flexibility adjustment of the VALCOE was not calculated in this study, mainly due to the combination of the meager documentation and time constraints. The main concerns are the parameters F_x and B_x in equation 2.13, the flexibility value multiplier and the base flexibility

value. Those terms are equivalent to the capacity credit and capacity value in the capacity adjustment calculations. F_x is, just as the capacity value, a number between 0 and 1, with a higher score for flexible power plants. The flexibility value should therefore be calculated using ramp-up times, storage present and the ability to turn off. Starting points could be MacDougall et al. (2013). The quantification of flexibility is a topic currently researched in the context of demand response in buildings and for the charging of electrical vehicles. A proven method could be taken from these areas as well. A starting point could be Finck et al. (2018) and Develder et al. (2016).

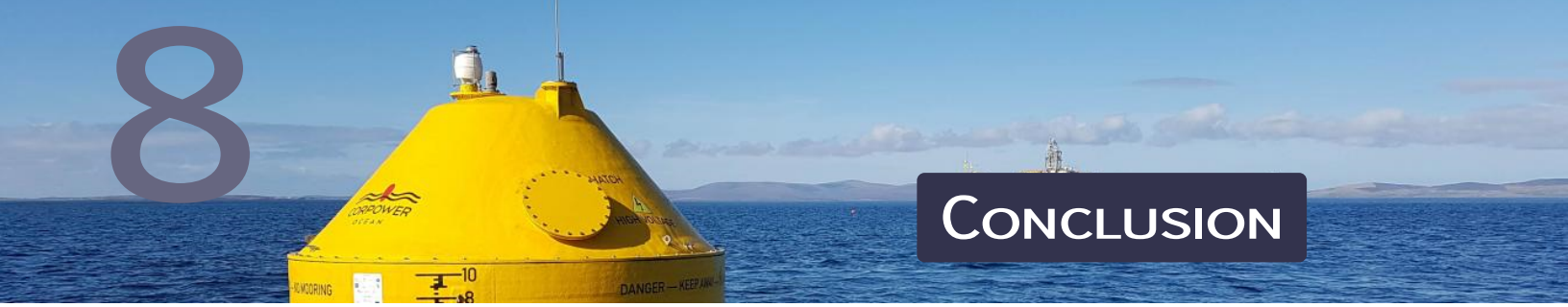

In this research, a techno-economic analysis is done on seven WECs using wave climate data from Lysekil (Sweden) and WaveHub (the UK), and Malta as a case study on a smaller energy system. The calculated LCOEs are in general higher than those of other energy technologies, and pay-back periods are longer than the lifetime of the single WEC devices at Lysekil. The PBP is reached within the lifetime for four of the seven devices deployed at the WaveHub site. The power matrices used predict a lower power output compared to most power matrices found in the literature. Also, methods to enhance power absorption are not considered, and cost savings from installing the WECs in parks has been considered for the Bref-HB device on one location, Lysekil.

According to this study, the WaveHub site is a more economically suitable site to deploy the WECs compared to Lysekil. In this work, only the positive aspects of the more energetic wave climate at WaveHub have been taken into account, and the expected higher costs due to for example a higher unavailability have been neglected. Including different costs for the two sites would give a more even result for the two sites.

The value adjustment is for all devices on all locations positive. This highlights that wave energy produces power during hours when the day ahead prices, and therefore electricity demand, are high. The capacity adjustment shows that the electricity systems in Sweden and the UK are extremely resilient, and adding a WEC to the systems will almost have no effect on the system-adequacy. The variability of wave energy power production is for both countries considerably lower compared to wind power and solar PV generation.

Further research could repeat such an analysis, but by replacing the power matrices with hydrodynamic calculations to directly obtain the power production, and consider wave parks of the other devices as well. Also, since there is a large uncertainty in the CAPEX and OPEX values, such an analysis could also be done for one specific WEC with CAPEX and OPEX material provided by the developers, and by considering several of those systems in a park, and by considering different OPEX values at different sites. Furthermore, it would be interesting to see if the same results of the Z-method would be obtained by using computationally expensive energy system models, to verify the application of the Z-method on wave energy. Finally, more research can be done in the development of the flexibility adjustment, and the definition of the flexibility multiplier and base flexibility value.

9 Acknowledgements

First and foremost I would like to thank Malin Göteman and Madeleine Gibescu for their support and feedback, for keeping their enthusiasm up on all new things I kept firing at them in my weekly updates. Also, it was not an easy task to arrange to write a master thesis abroad during Covid-19 times, and I am very grateful for their supportive attitude and for thinking with me on these matters as well. Specifically I want to thank Malin for the encouragement and support to work to a publication for the European Wave and Tidal Energy Conference.

I would also like to thank Veijo Pohjola and Ward van Pelt for keeping me a part of the Earth Sciences department at Uppsala Univeristy, by providing me with office space, a desktop, a job as research assistant and teacher, and occasionally for the refreshing football matches.

A lot of work has been spared me by Joana van Nieuwkoop and Aurélien Babarit, because they send me at the beginning of the research their datasets on respectively the sea states of WaveHub and the power matrices, for which I am eternally grateful. I also wish to thank George Lavidas for his comments on the Research Proposal, and Chris ten Dam for a very thorough final read and the resulting load of feedback!

References

Aderinto, Tunde and Li, Hua (2018). "Ocean wave energy converters: Status and challenges". In: *Energies* 11.5, p. 1250.

Astariz, S and Iglesias, G (2015). "The economics of wave energy: A review". In: *Renewable and Sustainable Energy Reviews* 45, pp. 397–408.

– (2016a). "Output power smoothing and reduced downtime period by combined wind and wave energy farms". In: *Energy* 97, pp. 69–81.

– (2016b). "Wave energy vs. other energy sources: A reassessment of the economics". In: *International Journal of Green Energy* 13.7, pp. 747–755.

Babarit, Aurélien, Hals, Jorgen, Muliawan, Made Jaya, Kurniawan, Adi, Moan, Torgeir, and Krokstad, Jorgen (2012). "Numerical benchmarking study of a selection of wave energy converters". In: *Renewable energy* 41, pp. 44–63.

Biyela, Siyanda S and Cronje, Willie A (2016). "Techno-Economic Analysis Framework for Wave Energy Conversion Schemes under South African Conditions: Modeling and Simulations". In: *International Journal of Energy and Power Engineering* 10.6, pp. 786–792.

Blanco, Marta Poncela, Spisto, Amanda, Hrelja, Nikola, and Fulli, Gianluca (2016). "Generation adequacy methodologies review". In: *JRC Science for Policy Report*.

Blok, Kornelis and Nieuwlaar, Evert (2016). *Introduction to energy analysis*. Taylor & Francis.

Booij, N, Holthuijsen, LH, and Ris, RC (1997). "The" SWAN" wave model for shallow water". In: *Coastal Engineering 1996*, pp. 668–676.

Borgarino, Bruno, Babarit, Aurélien, and Ferrant, Pierre (2012). "Impact of wave interactions effects on energy absorption in large arrays of wave energy converters". In: *Ocean Engineering* 41, pp. 79–88.

Brännlund, Runar and Vesterberg, Mattias (2018). "Peak and off-peak demand for electricity: subsistence levels and price elasticities". In: *Available at SSRN 3194465*.

Broberg, Thomas, Brännlund, Runar, and Persson, Lars (2017). "Consumer preferences and soft load control on the Swedish electricity market". In:

Bugeja, S (2020). "Hybrid Floating Wind and Solar Plants for Small Island States and Remote Communities: Synergy or Wishful Thinking? An Exploratory Study on the Maltese Islands." MA thesis.

Carnegie (Nov. 2020). *Carnegie, CETO WEC*. URL: https://www.carnegiece.com/technology/.

Castro-Santos, Laura, Garcia, Geuffer Prado, Estanqueiro, Ana, and Justino, Paulo APS (2015). "The Levelized Cost of Energy (LCOE) of wave energy using GIS based analysis: The case study of Portugal". In: *International Journal of Electrical Power & Energy Systems* 65, pp. 21–25.

Chang, Grace, Jones, Craig A, Roberts, Jesse D, and Neary, Vincent S (2018a). "A comprehensive evaluation of factors affecting the levelized cost of wave energy conversion projects". In: *Renewable Energy* 127, pp. 344–354.

Chang, Grace, Jones, Craig Alexander, and Roberts, Jesse (2018b). "A techno-economic analysis of wave energy conversion for the United States Pacific coast". In: *2018 Ocean Sciences Meeting*. AGU.

Chozas, Julia Fernandez, Kofoed, Jens Peter, and Sørensen, Hans Christian (2013). "Predictability and Variability of Wave and Wind: wave and wind forecasting and diversified energy systems in the Danish North Sea". In:

Clément, Alain, McCullen, Pat, Falcão, António, Fiorentino, Antonio, Gardner, Fred, Hammarlund, Karin, Lemonis, George, Lewis, Tony, Nielsen, Kim, Petroncini, Simona, et al. (2002). "Wave energy in Europe: current status and perspectives". In: *Renewable and sustainable energy reviews* 6.5, pp. 405–431.

Clemente, Daniel, Rosa-Santos, P, and Taveira-Pinto, F (2020). "On the potential synergies and applications of wave energy converters: A review". In: *Renewable and Sustainable Energy Reviews* 135, p. 110162.

CorPower (Sept. 2020). *CorPower, clean energy from our oceans*. URL: https://www.corpowerocean.com/.

Dalton, Gordon J, Alcorn, Raymond, and Lewis, T (2010). "Case study feasibility analysis of the Pelamis wave energy convertor in Ireland, Portugal and North America". In: *Renewable Energy* 35.2, pp. 443–455.

De Andres, Adrian, Maillet, Jéromine, Hals Todalshaug, Jørgen, Möller, Patrik, Bould, David, and Jeffrey, Henry (2016). "Techno-economic related metrics for a wave energy converters feasibility assessment". In: *Sustainability* 8.11, p. 1109.

Develder, Chris, Sadeghianpourhamami, Nasrin, Strobbe, Matthias, and Refa, Nazir (2016). "Quantifying flexibility in EV charging as DR potential: Analysis of two real-world data sets". In: *2016 IEEE International Conference on Smart Grid Communications (SmartGridComm)*. IEEE, pp. 600–605.

Diaz-Santamaria, Amaia, Cassar, Christopher-John, and Topham-Gonzalez, Eva (Mar. 2014). *Analysis of Cost Reduction Opportunities in the Wave Energy Industry*. URL: http://www.esru.strath.ac.uk/EandE/Web_sites/14-15/Wave_Energy/deliverables.html.

Dragoon, K and Dvortsov, V (2006). "Z-method for power system resource adequacy applications". In: *IEEE Transactions on Power Systems* 21.2, pp. 982–988.

Drew, Benjamin, Plummer, Andrew R, and Sahinkaya, M Necip (2009). *A review of wave energy converter technology*.

Energimyndigheten (Sept. 2019). *Energiläget*. URL: http://www.energimyndigheten.se/statistik/energilaget/?currentTab=1#mainheading.

Ericsson, Emil and Gregorson, Eric (2018). *Quantitative risk assessment of wave energy technology*.

Falcão, A (2009). *Renewable and Sustainable Energy Reviews. Wave Energy Utilization: A review of the technologies*.

Falnes, Johannes (2007). "A review of wave-energy extraction". In: *Marine structures* 20.4, pp. 185–201.

Finck, Christian, Li, Rongling, Kramer, Rick, and Zeiler, Wim (2018). "Quantifying demand flexibility of power-to-heat and thermal energy storage in the control of building heating systems". In: *Applied Energy* 209, pp. 409–425.

Fonseca, FX Correia da, Gomes, RPF, Henriques, JCC, Gato, LMC, and Falcao, AFO (2016). "Model testing of an oscillating water column spar-buoy wave energy converter isolated and in array: Motions and mooring forces". In: *Energy* 112, pp. 1207–1218.

Footprint, Carbon (June 2019). *CARBON FOOTPRINT COUNTRY SPECIFIC ELECTRICITY GRID GREENHOUSE GAS EMISSION FACTORS*. URL: https://www.carbonfootprint.com/docs/2019_06_emissions_factors_sources_for_2019_electricity.pdf.

Frew, Bethany A (2017). *Assessing Capacity Value of Wind Power*. Tech. rep. National Renewable Energy Lab.(NREL), Golden, CO (United States).

Giassi, Marianna, Castellucci, Valeria, Engström, Jens, Göteman, Malin, et al. (2019). "An economical cost function for the optimization of wave energy converter arrays". In: *The 29th International Ocean and Polar Engineering Conference*. International Society of Offshore and Polar Engineers.

Giassi, Marianna, Castellucci, Valeria, and Göteman, Malin (2020a). "Economical layout optimization of wave energy parks clustered in electrical subsystems". In: *Applied Ocean Research* 101, p. 102274.

Giassi, Marianna, Engström, Jens, Isberg, Jan, and Göteman, Malin (2020b). "Comparison of Wave Energy Park Layouts by Experimental and Numerical Methods". In: *Journal of Marine Science and Engineering* 8.10, p. 750.

Giassi, Marianna and Göteman, Malin (2018). "Layout design of wave energy parks by a genetic algorithm". In: *Ocean Engineering* 154, pp. 252–261.

Göteman, Malin, Engström, Jens, Eriksson, Mikael, and Isberg, Jan (2015). "Fast modeling of large wave energy farms using interaction distance cut-off". In: *Energies* 8.12, pp. 13741–13757.

Göteman, Malin, Engström, Jens, Eriksson, Mikael, Isberg, Jan, and Leijon, Mats (2014). "Methods of reducing power fluctuations in wave energy parks". In: *Journal of Renewable and Sustainable Energy* 6.4, p. 043103.

GOV.UK (Sept. 2020). *Historical time series data*. URL: https://www.gov.uk/government/collections/electricity-statistics#historical-time-series-data.

GOV.uk (Mar. 2019). *Collection: Capacity Market*. URL: https://www.gov.uk/government/collections/electricity-market-reform-capacity-market.

– (Nov. 2020). *Capacity Market UK collection*. URL: https://www.gov.uk/government/collections/electricity-market-reform-capacity-market.

Government Offices of Sweden (Feb. 2018). *Swedish Carbon Tax*. URL: https://www.government.se/government-policy/taxes-and-tariffs/swedens-carbon-tax/.

Graham, P. (2018). *Review of alternative methods for extending LCOE calculations to include balancing costs*.

Gunn, Kester and Stock-Williams, Clym (2012). "Quantifying the global wave power resource". In: *Renewable Energy* 44, pp. 296–304.

IEA (2018). *World Energy Outlook 2018*. URL: https://www.https://www.iea.org/reports/world-energy-outlook-2018.

– (2019). *World Energy Model Documentation 2019 version*. URL: https://iea.blob.core.windows.net/assets/d496ff6a-d4ca-4f6a-9471-220adddf0efd/WEM_Documentation_WEO2019.pdf.

– (Oct. 2020a). *World Energy Model Documentation 2020*. Tech. rep. IEA.

– (Apr. 2020b). *World Key Energy Statistics*. URL: https://www.iea.org/world.

Janssen, Peter and Janssen, Peter AEM (2004). *The interaction of ocean waves and wind*. Cambridge University Press.

Keane, Andrew, Milligan, Michael, Dent, Chris J, Hasche, Bernhard, D'Annunzio, Claudine, Dragoon, Ken, Holttinen, Hannele, Samaan, Nader, Soder, Lennart, and O'Malley, Mark (2010). "Capacity value of wind power". In: *IEEE Transactions on Power Systems* 26.2, pp. 564–572.

Korres, Gerasimos, Ravdas, Michalis, and Zacharioudaki, Anna (2019). "Mediterranean Sea Waves Analysis and Forecast (CMEMS MED-Waves)". In: *Copernicus Marine Service*.

Langlee (Nov. 2020). *Langlee wave power*. URL: http://www.langleewp.com/.

Lavelle, John and Kofoed, Jens Peter (2011). "Experimental testing of the Langlee wave energy converter". In: *Proceedings of the 9th European Wave and Tidal Energy Conference, Southampton, UK*.

Leijon, Mats, Boström, Cecilia, Danielsson, Oskar, Gustafsson, Stefan, Haikonen, Kalle, Langhamer, Olivia, Strömstedt, Erland, Stålberg, Magnus, Sundberg, Jan, Svensson, Olle, et al. (2008). "Wave energy from the North Sea: Experiences from the Lysekil research site". In: *Surveys in geophysics* 29.3, pp. 221–240.

Lejerskog, Erik, Boström, Cecilia, Hai, Ling, Waters, Rafael, and Leijon, Mats (2015). "Experimental results on power absorption from a wave energy converter at the Lysekil wave energy research site". In: *Renewable energy* 77, pp. 9–14.

Leskinen, Niina, Vimpari, Jussi, and Junnila, Seppo (2020). "Using real estate market fundamentals to determine the correct discount rate for decentralised energy investments". In: *Sustainable Cities and Society* 53, p. 101953.

MacDougall, Pamela, Roossien, Bart, Warmer, Cor, and Kok, Koen (2013). "Quantifying flexibility for smart grid services". In: *2013 IEEE Power & Energy Society General Meeting*. IEEE, pp. 1–5.

McGlade, Christophe and Ekins, Paul (2015). "The geographical distribution of fossil fuels unused when limiting global warming to 2 C". In: *Nature* 517.7533, pp. 187–190.

Mercados, AF (2016). "E-Bridge REF-E Identification of appropriate generation and system adequacy standards for the internal electricity market". In: *Final report prepared for the European Commission*.

Mérigaud, Alexis and Ringwood, John V (2018). "Power production assessment for wave energy converters: Overcoming the perils of the power matrix". In: *Proceedings of the Institution of Mechanical Engineers, Part M: Journal of Engineering for the Maritime Environment* 232.1, pp. 50–70.

National Grid (Sept. 2020). *The National Grid*. URL: https://www.nationalgrid.com/uk/electricity-transmission/.

Nexans (May 2020). *Nexans completes repair of Malta-Sicily subsea interconnector*. URL: https://www.nexans.com/newsroom/news/details/2020/05/nexans-completes-repair-malta-sicily-subsea-interconnector.html#:~:text=The%5C%20Interconnector%5C%20cable%5C%20was%5C%20damaged,the%5C%20nature%5C%20of%5C%20the%5C%20fault..

Nieuwkoop, Joana CC van, Smith, Helen CM, Smith, George H, and Johanning, Lars (2013). "Wave resource assessment along the Cornish coast (UK) from a 23-year hindcast dataset validated against buoy measurements". In: *Renewable energy* 58, pp. 1–14.

Nordpool (Oct. 2020). *Historical Market Data*. URL: https://www.nordpoolgroup.com/historical-market-data/.

O'Connor, Michael, Lewis, T, and Dalton, Gordon (2013). "Operational expenditure costs for wave energy projects and impacts on financial returns". In: *Renewable Energy* 50, pp. 1119–1131.

Ocean Energy Ireland (Nov. 2020). *Ocean Energy Ireland*. URL: https://www.oceanenergyireland.com/.

OECD (Nov. 2019). *Global Feed-in Tarifs Table*. URL: https://stats.oecd.org/Index.aspx?DataSetCode=RE_FIT.

Office for National Statistics (Sept. 2020). *Office for National Statistics*. URL: https://www.ons.gov.uk/.

Ofgem (Nov. 2020). *Environmental Programs*. URL: https://www.ofgem.gov.uk/environmental-programmes.

Oliveira-Pinto, Sara, Rosa-Santos, Paulo, and Taveira-Pinto, Francisco (2019). "Electricity supply to offshore oil and gas platforms from renewable ocean wave energy: Overview and case study analysis". In: *Energy Conversion and Management* 186, pp. 556–569.

– (2020). "Assessment of the potential of combining wave and solar energy resources to power supply worldwide offshore oil and gas platforms". In: *Energy Conversion and Management* 223, p. 113299.

OPSD (Oct. 2020). *Open Power System Data - A free and open data platform for power system modelling*. URL: https://open-power-system-data.org/.

Pecher, Arthur (2012). *Performance evaluation of wave energy converters*. River Publishers.

Pihl, Hjalmar (2019). “Swedish FCR prices-an analysis of the data”. In: *Energy Economics Lab, Tech. Rep., nov*.

Piscopo, V, Benassai, G, Della Morte, R, and Scamardella, A (2017). “Towards a cost-based design of heaving point absorbers”. In: *International journal of marine energy* 18, pp. 15–29.

Pontoon (Nov. 2020). *Pontoon power*. URL: https://www.pontoon.no/.

Previsic, Mirko, Epler, Jeff, Hand, Maureen, Heimiller, Donna, Short, Walter, and Eurek, Kelly (2012). *The future potential of waver power in the United States*. Tech. rep. Re Vision Consulting, LLC, Sacramento, California.

Quitoras, Marvin Rhey D, Abundo, Michael Lochinvar S, and Danao, Louis Angelo M (2018). “A techno-economic assessment of wave energy resources in the Philippines”. In: *Renewable and Sustainable Energy Reviews* 88, pp. 68–81.

Ruiz, Pau Mercadé, Nava, Vincenzo, Topper, Mathew BR, Minguela, Pablo Ruiz, Ferri, Francesco, and Kofoed, Jens Peter (2017). “Layout optimisation of wave energy converter arrays”. In: *Energies* 10.9, p. 1262.

Salmon, Rick (2008). “Introduction to ocean waves”. In: *Scripps Institution of Oceanography, University of California, San Diego*.

SCB (Sept. 2020). *SCB*. URL: https://www.scb.se/.

Seabased (Nov. 2020). *SEABASED WEC*. URL: https://seabased.com/.

Sheng, Wanan (2019a). “Power performance of BBDB OWC wave energy converters”. In: *Renewable Energy* 132, pp. 709–722.

– (2019b). “Wave energy conversion and hydrodynamics modelling technologies: A review”. In: *Renewable and Sustainable Energy Reviews* 109, pp. 482–498.

Söder, Lennart, Tómasson, Egill, Estanqueiro, Ana, Flynn, Damian, Hodge, Bri-Mathias, Kiviluoma, Juha, Korpås, Magnus, Neau, Emmanuel, Couto, António, Pudjianto, Danny, et al. (2020). “Review of wind generation within adequacy calculations and capacity markets for different power systems”. In: *Renewable and Sustainable Energy Reviews* 119, p. 109540.

Svenska Kraftnät (Nov. 2017). *System Development Plan 2018 - 2027*. URL: https://www.svk.se/siteassets/om-oss/rapporter/2018/svenska-kraftnat-system-development-plan-2018-2027.pdf.

– (Mar. 2018). *The Way forward - Solutions for a changing Nordic power system*. Tech. rep. Statnett, FinGrid, Energinet, Svenska Kraftnät.

– (Sept. 2020). *Svenska Kraftnät*. URL: https://www.svk.se/.

Swedish Energy Agency (2019). *The Swedish-Norwegian Electricity Certificate Market ANNUAL REPORT 2018*. Tech. rep. Swedish Energy Agency.

Teillant, Boris, Costello, Ronan, Weber, Jochem, and Ringwood, John (2012). “Productivity and economic assessment of wave energy projects through operational simulations”. In: *Renewable Energy* 48, pp. 220–230.

Ulazia, Alain, Penalba, Markel, Ibarra-Berastegui, Gabriel, Ringwood, John, and Saénz, Jon (2017). "Wave energy trends over the Bay of Biscay and the consequences for wave energy converters". In: *Energy* 141, pp. 624–634.

Vesterberg, Mattias (2016). "The hourly income elasticity of electricity". In: *Energy Economics* 59, pp. 188–197.

Wang, Liguo, Engström, Jens, Göteman, Malin, and Isberg, Jan (2015). "Constrained optimal control of a point absorber wave energy converter with linear generator". In: *Journal of renewable and sustainable energy* 7.4, p. 043127.

Waters, Rafael, Engström, Jens, Isberg, Jan, and Leijon, Mats (2009). "Wave climate off the Swedish west coast". In: *Renewable Energy* 34.6, pp. 1600–1606.

WaveStar (Nov. 2020). *Wavestar energy*. URL: http://wavestarenergy.com/.

Welsch, Manuel, Howells, Mark, Hesamzadeh, Mohammad Reza, Ó Gallachóir, Brian, Deane, Paul, Strachan, Neil, Bazilian, Morgan, Kammen, Daniel M, Jones, Lawrence, Strbac, Goran, et al. (2015). "Supporting security and adequacy in future energy systems: The need to enhance long-term energy system models to better treat issues related to variability". In: *International Journal of Energy Research* 39.3, pp. 377–396.

Widén, Joakim, Carpman, Nicole, Castellucci, Valeria, Lingfors, David, Olauson, Jon, Remouit, Flore, Bergkvist, Mikael, Grabbe, Mårten, and Waters, Rafael (2015). "Variability assessment and forecasting of renewables: A review for solar, wind, wave and tidal resources". In: *Renewable and Sustainable Energy Reviews* 44, pp. 356–375.

Wu, Junhua, Shekh, Slava, Sergiienko, Nataliia Y, Cazzolato, Benjamin S, Ding, Boyin, Neumann, Frank, and Wagner, Markus (2016). "Fast and effective optimisation of arrays of submerged wave energy converters". In: *Proceedings of the Genetic and Evolutionary Computation Conference 2016*, pp. 1045–1052.

Xu, Xinxin, Robertson, Bryson, and Buckham, Bradley (2020). "A techno-economic approach to wave energy resource assessment and development site identification". In: *Applied Energy* 260, p. 114317.